Functional analysis of cyclic diguanylate-modulating proteins in *Vibrio fischeri*

Ruth Y. Isenberg[1,2,4], Chandler S. Holschbach[1], Jing Gao[3], and Mark J. Mandel[1,2]*

[1] Department of Medical Microbiology and Immunology, University of Wisconsin-Madison, Madison, WI USA

[2] Microbiology Doctoral Training Program, University of Wisconsin-Madison, Madison, WI USA

[3] Department of Microbiology-Immunology, Northwestern University Feinberg School of Medicine, Chicago, IL USA

[4] Current address: Department of Microbiology and Immunology, University of Minnesota Medical School, Minneapolis, MN USA

Short title: Systems-level analysis of *V. fischeri* c-di-GMP genes

Keywords: *Vibrio fischeri*, c-di-GMP, flagellar motility, biofilm

* Correspondence to:

Mark J. Mandel
University of Wisconsin-Madison
Department of Medical Microbiology and Immunology
1550 Linden Drive
Madison, WI 53706
Phone: (608) 261-1170
Fax: (608) 262-8418
Email: mmandel@wisc.edu

ABSTRACT

As bacterial symbionts transition from a motile free-living state to a sessile biofilm state, they must coordinate behavior changes suitable to each lifestyle. Cyclic diguanylate (c-di-GMP) is an intracellular signaling molecule that can regulate this transition, and it is synthesized by diguanylate cyclase (DGC) enzymes and degraded by phosphodiesterase (PDE) enzymes. Generally, c-di-GMP inhibits motility and promotes biofilm formation. While c-di-GMP and the enzymes that contribute to its metabolism have been well-studied in pathogens, considerably less focus has been placed on c-di-GMP regulation in beneficial symbionts. *Vibrio fischeri* is the sole beneficial symbiont of the Hawaiian bobtail squid (*Euprymna scolopes*) light organ, and the bacterium requires both motility and biofilm formation to efficiently colonize. C-di-GMP regulates swimming motility and cellulose exopolysaccharide production in *V. fischeri*. The genome encodes 50 DGCs and PDEs, and while a few of these proteins have been characterized, the majority have not undergone comprehensive characterization. In this study, we use protein overexpression to systematically characterize the functional potential of all 50 *V. fischeri* proteins. All 28 predicted DGCs and 14 predicted PDEs displayed at least one phenotype consistent with their predicted function, and a majority of each displayed multiple phenotypes. Finally, active site mutant analysis of proteins with the potential for both DGC and PDE activities revealed potential activities for these proteins. This work presents a systems-level functional analysis of a family of signaling proteins in a tractable animal symbiont and will inform future efforts to characterize the roles of individual proteins during lifestyle transitions.

IMPORTANCE

C-di-GMP is a critical second messenger that mediates bacterial behaviors, and *V. fischeri* colonization of its Hawaiian bobtail squid host presents a tractable model in which to interrogate

the role of c-di-GMP during animal colonization. This work provides systems-level characterization of the 50 proteins predicted to modulate c-di-GMP levels. By combining multiple assays, we generated a rich understanding of which proteins have the capacity to influence c-di-GMP levels and behaviors. Our functional approach yielded insights into how proteins with domains to both synthesize and degrade c-di-GMP may impact bacterial behaviors. Finally, we integrated published data to provide a broader picture of each of the 50 proteins analyzed. This study will inform future work to define specific pathways by which c-di-GMP regulates symbiotic behaviors and transitions.

INTRODUCTION

Many bacteria exist in the environment in a free-living state, and upon encountering an animal host undergo dramatic developmental transitions. These adjustments enable symbiotic microbes–including mutualists, commensals, and pathogens–to acclimate to the physical, chemical, and nutritional milieu in the host; to resist immune responses; and to engage in behaviors required for survival and growth within the distinct host environment (1–5). To manage such transitions successfully, bacteria often inversely regulate motility and adhesion (6–11). In the motile state, it would be counterproductive to be adherent, and environmental bacteria use motility and chemotaxis to colonize novel niches, seek nutrition, and avoid predation (12–14). In contrast, adherent bacteria, especially those that have formed a multicellular biofilm, do not have a need for swimming motility. As a result there are multiple mechanisms that bacteria use to coordinately and inversely regulate these two broad behaviors (15–18). Alteration of the levels of the intracellular second messenger cyclic diguanylate (c-di-GMP) is a common mechanism used by bacteria to accomplish this purpose (19). In general, c-di-GMP promotes biofilm formation and inhibits motility (20). Enzymes that regulate c-di-GMP levels are diguanylate cyclases (DGCs), which synthesize c-di-GMP, and phosphodiesterases

(PDEs), which degrade the molecule. DGCs contain GGDEF domains with conserved GG(D/E)EF active site residues, while PDEs contain EAL domains with conserved ExLxR active site residues or HD-GYP domains with conserved HD and GYP active site residues (21–26). Although many proteins have both GGDEF and EAL domains, only one domain is usually active, even when the amino acid motif for the other domain should function based on sequence conservation (27–30). However, environmental conditions may influence whether some dual-function proteins exhibit primarily DGC or PDE activity (31).

Much of what is known about c-di-GMP regulation of biofilm, motility, and host colonization is from studies on pathogenic species (32–34). Activation of cellulose production was the first role defined for c-di-GMP, in *Acetobacter xylinum* (now *Komagataeibacter xylinus*), and has remained one of most well characterized c-di-GMP-regulated phenotypes across taxa (20, 21). C-di-GMP-mediated cellulose production has been implicated in host colonization defects by pathogens *Escherichia coli* and *Salmonella enterica* serovar Typhimurium (33). Although much focus has been placed on defining roles for c-di-GMP in pathogenic associations, recent studies have focused on the impacts of c-di-GMP in bacteria during beneficial host associations. Host-derived ligands inactivate *Aeromonas veronii* DGC SpeD, which promotes host colonization (35). Additionally, high levels of c-di-GMP negatively impact the establishment of the symbiosis between the bioluminescent marine bacterium *Vibrio fischeri* and its host the Hawaiian bobtail squid (*Euprymna scolopes*) (36). *V. fischeri* is the sole, beneficial light organ symbiont of the Hawaiian bobtail squid (*Euprymna scolopes*), and the bacterium requires both swimming motility and biofilm formation to successfully colonize the host light organ (37–40). *V. fischeri* express polar flagella in seawater and form biofilm aggregates in the host mucus before migrating into the light organ (37, 38, 41–44). *V. fischeri* produce cellulose via the *bcs* locus-encoded cellulose synthase enzyme, which is activated by c-di-GMP, and genetic manipulation of c-di-GMP levels through deletion or overexpression of DGCs and PDEs modulates cellulose production (39, 45–

48). Although cellulose is not required for symbiotic biofilm or squid colonization, an *in vivo* regulatory interaction exists between cellulose and the symbiosis polysaccharide (Syp) (36, 38, 39, 42, 49, 50).

We previously examined how global c-di-GMP levels impact bacterial behaviors in *V. fischeri*, including cellulose production, cellulose synthase and *syp* transcriptional reporter activities, and flagellar motility (36). For that work, we took advantage of a strain lacking seven DGCs and another strain lacking six PDEs to adjust the global c-di-GMP pool. That effort sparked our interest in the potential redundancy of the dozens of predicted c-di-GMP modulating enzymes and the capacity of the encoded proteins to impact bacterial behavior. It is common for bacteria, especially those with diverse lifestyles, to encode many DGCs and PDEs: *E. coli* encodes 29 such enzymes and *Vibrio cholerae* encodes 62 (51, 52). *V. fischeri* strain ES114 encodes 50 genes predicted to modulate c-di-GMP levels (**FIG. 1**) (53, 54). Of these possible c-di-GMP-modulating proteins, only a few have been characterized in depth for their roles in biofilm formation and/or swimming motility. DGCs MifA and MifB regulate magnesium-dependent motility by contributing to flagellar biogenesis (45). CasA is a DGC that is activated by calcium to inhibit motility and promote cellulose biofilm formation (48). Reduction of c-di-GMP levels by PDE BinA reduces cellulose synthesis (46). LapD has degenerate GGDEF and EAL active sites, one or both of which may recognize c-di-GMP to prevent cleavage of the biofilm-promoting adhesin LapV (47). In this model, the PDE PdeV activates biofilm dispersal by decreasing the c-di-GMP pool that activates LapD (47). In *V. fischeri* strain KB2B1, the ortholog of DGC VF_1200 was shown to inhibit swimming motility (55). The other 44 *V. fischeri* predicted c-di-GMP-modulating proteins have not undergone comprehensive phenotypic characterization, although a recent study was published where motility of c-di-GMP-modulating gene mutants were assessed (54). Additionally, none of the 50 c-di-GMP-modulating proteins have been shown to impact host colonization individually, although putative PDE VF_A0879 was predicted

to be required for host colonization in a transposon insertion sequencing study (56). In this report, we systematically dissected the capability of *V. fischeri* predicted c-di-GMP-modulating enzymes to impact various biofilm and motility phenotypes through an approach combining systems-level overexpression analysis and targeted active site mutations.

RESULTS

V. fischeri encodes 50 proteins predicted to modulate c-di-GMP levels

The *V. fischeri* genome (strain ES114) encodes 50 proteins containing DGC and/or PDE domains (49, 50, 53, 54). Twenty-eight are predicted DGCs with GGDEF domains, 14 are predicted PDEs (12 with EAL domains, 2 with HD-GYP domains), 5 are predicted dual-function proteins with both GGDEF and EAL domains, and 3 are predicted to be nonfunctional due to degenerate active sites. The genes encoding these proteins are spread across both *V. fischeri* chromosomes, with most (31 out of 50) of the genes located on the smaller second chromosome (**FIG. 1**). To further characterize the functions of all 50 proteins, we took an overexpression approach to examine the function of each protein when individually overexpressed in *V. fischeri*. We sought this approach to be resilient against the redundancy we expect to exist within the large gene families. A similar overexpression approach has been effective to evaluate phenotypes of DGCs and PDEs in *V. cholerae* (57–61) and in other bacteria (28, 62–64). We used an IPTG-inducible vector to overexpress each protein in *V. fischeri* and performed assays to quantify cellulose production, swimming motility, and c-di-GMP levels. We also included control strains overexpressing VC1086 (a *V. cholerae* PDE) and QrgB (a *Vibrio campbellii* BB120 DGC), which have served as effective controls in multiple organisms (59, 61, 64–69). We note that the vector backbone used is the same as in many of the *V.*

cholerae studies. Assays were conducted in a 96-well format to facilitate simultaneous, reproducible assays of the complete set of 54 test and control strains.

Predicted *V. fischeri* DGCs and PDEs impact cellulose polysaccharide production

C-di-GMP promotes cellulose synthesis in many bacteria including *V. fischeri* (46, 48). To assess cellulose production across the set of proteins, we performed Congo red binding assays (46) of strains overexpressing each protein. Most DGCs (17/28 *V. fischeri* DGCs) increased cellulose production, consistent with their predicted function, including characterized DGCs MifA and CasA (**FIG. 2A**). Known *V. campbellii* DGC QrgB also increased cellulose production (**FIG. 2A**). The increase in cellulose production upon overexpression of known DGC MifA is consistent with published results (45), and the CasA overexpression result is consistent with data showing decreased cellulose production in a Δ*casA* strain (48). While overexpression of the remaining predicted DGCs did not significantly alter Congo red binding levels, many had a trend in the positive direction as expected and consistent with an increase in c-di-GMP levels (**FIG. 2A**).

Overexpression of 9/14 predicted PDEs significantly decreased cellulose production upon overexpression, consistent with their predicted function, including characterized PDE BinA. Known *V. cholerae* PDE VC1086 also decreased cellulose production (**FIG. 2A**). Our results are consistent with published results showing effects on cellulose production for PDE BinA (46, 47).

V. fischeri encodes five proteins with both GGDEF and EAL domains. Proteins that contain both GGDEF and EAL domains typically only have one domain exhibit activity, even if the amino acid motif for the other domain is conserved (27–30), though there is evidence of a dual-function protein capable of exhibiting either DGC or PDE activity depending on conditions (31). We therefore expected these dual-function proteins to behave predominantly as DGCs or PDEs. Of

the five predicted dual-function proteins, overexpression of VF_0985 increased cellulose production while VF_0094 and VF_0494 decreased cellulose production compared to the empty vector control (**FIG. 2A**).

Finally, we examined the three predicted "degenerate" c-di-GMP modulating enzymes; i.e., proteins with intact GGDEF and/or EAL domains but with degenerate GG(D/E)EF and/or ExLxR active site motifs that are not predicted to function. None of these proteins significantly impacted cellulose production (**FIG. 2A**).

Predicted *V. fischeri* DGCs and PDEs influence flagellar motility

As a second behavioral output of c-di-GMP levels, we proceeded to assay swimming motility in the same set of strains. We conducted swimming motility assays of strains overexpressing each protein in TBS soft agar and in TBS soft agar with the addition of either magnesium or calcium, which are known to influence swimming behavior by *V. fischeri* (54, 70). We observed that most DGCs (21/28) and 6/14 PDEs showed the expected overexpression results of inhibiting or promoting motility, respectively, including known *V. fischeri* DGCs MifA, MifB, and CasA and known PDE BinA (**FIG. 2B**). *V. campbellii* DGC QrgB and *V. cholerae* PDE VC1086 also showed the expected results (**FIG. 2B**). Overexpression of either DGC MifA, MifB, or CasA diminished motility under all conditions tested despite having known cation-specific motility phenotypes (**FIG. 2B; FIG. S1**). MifA and MifB inhibit motility in the presence of magnesium (45), while CasA inhibits motility in the presence of calcium (48), and we suspect that overexpression of the proteins likely amplified their respective DGC activities and bypassed the requirement for the respective cations. One example where we observed a media-specific effect is for VF_0985, which strongly inhibited motility upon overexpression in TBS and TBS-Ca, relative to the empty vector control, but not in TBS-Mg (**FIG. 2B; FIG. S1**).

Overexpression of predicted degenerate proteins VF_0355 and VF_A0216 did not significantly impact motility (**FIG. 2B; FIG. S1**). Overexpression of LapD decreased motility in two of the three motility media types (**FIG. 2B; FIG. S1**), but this is likely independent of c-di-GMP modulation and is consistent with the function of LapD in inhibiting biofilm dispersal (47), which is associated with decreased motility.

Expression level of *V. fischeri* proteins does not correlate with magnitude of phenotypes

Of the *V. fischeri* proteins assayed, 13 did not have significant phenotypes for either cellulose production or motility: DGCs CdgG, VF_1245, VF_1515, VF_A0056, VF_A0476, VF_A0796; PDEs VF_A0706, VF_A0879, VF_A1076, and PdeV; dual-function proteins VF_A0244 and VF_A0475; and predicted degenerate proteins VF_0355 and VF_A0216 (**FIG. 2; FIG. S1**). This result for these proteins could be due to lack of enzymatic activity under the conditions tested, or could be the result of posttranscriptional regulation that prevents these proteins from being expressed. To test whether the lack of significant phenotypes from these proteins was due to protein expression, we assessed expression of several FLAG-tagged proteins via western blot. We selected proteins with strong phenotypes in both the cellulose and motility assays (MifA, VF_A0057, and VF_A0155), one protein with a phenotype in just the motility assay (VF_A0342), proteins with no significant phenotypes in either assay (VF_1515, VF_A0056, and VF_A0476), and a predicted degenerate protein with no significant phenotypes (VF_A0216). All three proteins with strong phenotypes in both assays were expressed robustly (**FIG. 3**). Two of the proteins with no significant phenotypes (VF_A0056 and VF_A0476) were expressed, with the intensity of the band for VF_A0056 as strong as the bands for the proteins with significant phenotypes in both assays (**FIG. 3**). The predicted degenerate protein VF_A0216 was also expressed, as was VF_A0342 which only had a significant motility phenotype (**FIG. 3**).

VF_1515, which had no significant phenotypes, was the only protein tested that had no observable expression via western blot, suggesting that VF_1515 protein is not produced at a substantial level under the conditions tested (**FIG. 3**). Therefore, while we expect that most proteins expressed from pEVS143 are found at appreciable levels in the cell, including those proteins that do not yield detectable phenotypes, in at least one case we found that the protein assayed was not expressed stably in the cell. Further, the magnitude of the cellulose and motility phenotypes do not correlate with protein expression level for proteins that are expressed.

Predicted *V. fischeri* DGCs and PDEs modulate c-di-GMP reporter levels

Congo red and motility assays revealed that most of the *V. fischeri* DGCs and PDEs influence phenotypes associated with c-di-GMP. We next asked to what capacity these proteins are capable of modulating c-di-GMP levels using the pFY4535 fluorescent c-di-GMP reporter plasmid (71), which we used previously to quantify c-di-GMP levels in *V. fischeri* (36). We expected overexpression of DGCs to increase c-di-GMP levels and overexpression of PDEs to decrease c-di-GMP levels relative to the empty vector control. We also expected proteins with the strongest cellulose and/or motility phenotypes to have the strongest effects of c-di-GMP reporter activity. Consistent with their predicted function, overexpression of all 28 predicted DGCs increased c-di-GMP reporter activity, including characterized *V. fischeri* DGCs MifA and MifB (**FIG. S2A**). The results for overexpression of MifA and MifB are consistent with published results (45). In contrast to the results with DGCs, upon overexpression only 4/14 predicted PDEs, VF_0087, VF_A0506, VF_A0526, and VF_A0706, had the expected effect of significantly decreasing c-di-GMP reporter activity (**FIG. S2A**). These results are also in contrast to the cellulose and motility results, where overexpression of the majority of PDEs elicited at least one of the expected phenotypes, and no PDEs had significant opposite cellulose or motility

phenotypes (**FIG. 2; FIG. S2D**). BinA is a characterized PDE that negatively influences c-di-GMP levels (absence of BinA resulted in increased c-di-GMP compared to WT) (46). Our results show that BinA overexpression diminished c-di-GMP reporter activity by 57%, but this result was not statistically significant (**FIG. S2A**). However, the cellulose and motility results for BinA are among the strongest of the PDEs (**FIG. 2; FIG. S2D**). Similarly, overexpression of known *V. cholerae* PDE VC1086 also did not significantly alter c-di-GMP reporter activity (**FIG. S2A**), but did significantly alter cellulose production and motility in the expected directions (**FIG. 2; FIG. S2D**). Surprisingly, five predicted PDEs, VF_0091, VF_1367, VF_A0344, and VF_A0879, and VF_A1076 significantly increased c-di-GMP reporter activity upon overexpression (**FIG S2A**). The same results were observed when the strains were assayed individually rather than in the arrayed 96-well format, with the exception of VF_1367 which did not have significant results in the individual assay format (**FIG. S2B**). Of these five PDEs, VF_0091 significantly decreased cellulose production and none significantly increased motility, but these phenotypes do not correspond with increased c-di-GMP reporter activity (**FIG. 2; FIG. S2D**). One interpretation of these results is that the c-di-GMP reporter reports a local level of c-di-GMP while the Congo red and motility assays report global levels. Local c-di-GMP levels measured by the reporter may correspond with global levels for the majority of strains, but not for strains overexpressing some PDEs, where the dynamic range of c-di-GMP levels is much more limited and local pools may be subject to substantial variation from the global dynamics. We previously reported that in a high c-di-GMP strain of *V. fischeri*, overexpression of PDE VC1086 reduced c-di-GMP reporter activity 1.6-fold when measured with the same reporter (36). However, overexpression with the same vector in wild-type *V. fischeri* had no effect on the already-low c-di-GMP reporter activity. Therefore, while the c-di-GMP reporter levels were well-correlated with c-di-GMP-responsive phenotypes for the DGCs, data from the reporter were not informative for predicting phenotypes from the low basal wild-type levels. To test whether the pFY4535 c-di-GMP biosensor could better report decreased c-di-GMP in a high c-di-GMP background, we overexpressed select

PDEs in a strain of *V. fischeri* deleted for six PDEs (Δ6PDE) and has been demonstrated to have high basal c-di-GMP levels (36). Every PDE tested diminished c-di-GMP reporter activity in the high c-di-GMP background, including VF_0091 and VF_A1076, which exhibited the highest reporter activity in the wild-type background (**FIG. S2C**). Dual-function protein VF_0094 diminished reporter activity comparable to the strongest PDE in the assay (**FIG. S2C**), consistent with the cellulose and motility results for this protein in the wild-type background (**FIG. 2**). To further probe the accuracy of the c-di-GMP reporter for functional characterization of DGC and PDE activities, we selected several PDE overexpression strains to measure c-di-GMP levels using a commercially available ELISA kit. The results of the ELISA c-di-GMP quantification did not agree with the phenotypic characterization of the selected PDEs, nor did they agree with the c-di-GMP reporter data (**FIG. S3**). We also quantified the phenotypic correlation of the reporter data with our Congo red ($R^2 = 0.69$) and motility ($R^2 = 0.66$) results, which was lower in both cases than the correlation of the Congo red and motility phenotypes to each other ($R^2 = 0.77$). Given these questions about the utility of the reporter activity in the wild-type background when c-di-GMP levels are diminished, for our overall question of the catalytic potential of the proteins assayed we argue that in this case it is most prudent to infer global c-di-GMP-dependent processes from the phenotypic assays of cellulose production and swimming motility. In the next section, we test this hypothesis through mutation of relevant c-di-GMP active sites.

Select *V. fischeri* DGCs and PDEs impact motility and biofilm phenotypes through their c-di-GMP catalytic sites

Most of the DGCs and PDEs exhibited the expected cellulose and motility phenotypes upon overexpression (**FIG. 2**). If the results we observed were due to catalytic function, then mutation of the active sites should impact these phenotypes. Changing the second amino acid in the

GGDEF motif to A (62, 72, 73) drastically reduced the effects of MifA, VF_A0057, VF_A0152, and VF_A0398 on cellulose production and motility (**FIG. 4**). These results confirm that intact GGDEF domains are required for the regulatory functions of these proteins.

VF_A0057 is one of the more interesting predicted DGCs because it has a non-consensus GGDEF domain with a serine instead of a glycine in the first position of the motif (i.e., SGDEF). The altered motif is not functional in *V. cholerae* CdgG, which led us to predict it to be similarly nonfunctional in *V. fischeri* VF_A0057 (72). Surprisingly, though, mutation of the second amino acid of the motif in VF_A0057, resulting in the amino acid sequence SADEF, substantially mitigated the effects of the protein on cellulose production and motility, suggesting that the non-canonical SDGEF motif in this protein is functional and that VF_A0057 likely has DGC activity (**FIG. 4**). CdgG, a homolog of the nonfunctional *V. cholerae* protein CdgG, is another predicted DGC with a non-consensus active site where the first amino acid is a serine: SGEEF. However, overexpression of CdgG or the variant (SAEEF) did not promote cellulose production or inhibit motility (**FIG. 4**).

To examine the catalytic site of the PDEs, we similarly replaced the first residue of the ExLxR motif with an alanine, a mutation that has been used previously to disrupt EAL domain activity (46, 59, 74, 75). AxLxR mutants of BinA and VF_0087 attenuated the effects of these proteins on cellulose production and motility (**FIG. 4**). These results confirm previous work (46, 54, 55), and are the first demonstration of the requirement for the active site residues for VF_0087 function.

VF_1367 is one of two predicted HD-GYP domain PDEs encoded by *V. fischeri*. The motif encoded is HD-GYL, but the presumed HD catalytic dyad for HD superfamily proteins is still intact (23). Here, we changed the second amino acid to an alanine, which has been used to

disrupt HD-GYP domain activity (25, 60). Overexpression of an HA-GYL variant of VF_1367 obviated the impact on cellulose production, which was the major phenotype observed on overexpression of the wild-type protein (**FIG. 4**). Overexpression of active site mutants of predicted and characterized DGCs and PDEs thus supports the predicted biochemical activities of individual proteins and validates our overall approach of overexpressing predicted c-di-GMP-modulating proteins to understand the genome-wide functional landscape.

Challenges in assigning functions for dual-domain proteins

Three of the five *V. fischeri* dual-function proteins had clear phenotypes in both cellulose production and motility assays, suggesting they may primarily function as DGCs or PDEs (**FIG. 2**). However, overexpression of proteins with both GGDEF and EAL domains can only hint at whether a protein primarily has DGC or PDE activity and does not discern which domains are active/inactive. To assess whether one, both, or neither of the DGC and PDE domains contribute to the effects of these predicted dual-domain protein, we assayed strains overexpressing GGDEF mutants, EAL mutants, or GGDEF/EAL double mutants of each protein. As one example, phenotypic assays strongly suggested that VF_0985 behaved as a DGC given its impact on cellulose and motility (**FIG. 2**). A VF_0985 AAL mutant behaved like the wild-type protein in all assays when overexpressed, while a GADEF mutant drastically reduced the effects of VF_0985 on cellulose production and motility (**FIG. 5**). Interestingly, mutation of the GGDEF domain seemed to reverse the effects of VF_0985: the GGDEF mutant behaved similar to a PDE in both assays (**FIG. 5**), suggesting the EAL domain may be active. When the VF_0985 double GADEF/AAL mutant was overexpressed, cellulose production resembled the single GGDEF mutant, while little effect on motility was observed (**FIG. 5**). These results suggest that, under the conditions tested, VF_0985 likely functions predominantly as a DGC, but that we may be detecting cryptic PDE activity in the variant in which DGC activity is absent. Active site

mutant analysis of the remaining four dual-function proteins similarly suggest a more complicated picture than one dominant domain. Further in-depth studies of these proteins will be required to dissect their roles in cellulose production and motility, and the mechanisms by which these proteins perform those roles.

DISCUSSION

V. fischeri is an emerging model for studies of c-di-GMP regulation, and especially for how c-di-GMP impacts animal host colonization. We previously demonstrated that high global levels of c-di-GMP impair colonization, though it is unknown how levels remain low to facilitate a productive host-microbe symbiosis. An ongoing goal is to elucidate relevant signaling that enables proper c-di-GMP in the host and during transitions to and from the host-associated state. Therefore, the goal of the current study was to identify which of the predicted 50 c-di-GMP modulating proteins–DGCs, PDEs, dual-function DGC/PDEs, and likely degenerate enzymes–are able to elicit c-di-GMP-responsive phenotypes in *V. fischeri*. In **Figure 6** we assembled the results from our analyses to demonstrate cellulose production and swimming motility results for all 50 *V. fischeri* proteins and the two control proteins. Furthermore, we integrated data from a recent study (54) that examined swimming motility of single-gene mutants in the same *V. fischeri* proteins. The resulting table (**FIG. 6**) presents a powerful visualization of current knowledge of the catalytic potential of these gene families. Conducted in different labs, there is remarkable consistency among the results. There are more proteins with significant effects observed upon overexpression (32/50 in at least one motility assay) compared to gene deletion (20/50), which was expected, and supports our approach to use the overexpression approach to reveal function in a family where redundancy is expected. The one case in which discrepancies were noted were for DGC VF_A0368, where we had consistent results across all conditions and the deletion approach yielded significant results only on TBS swim plates. The only cases in which

a phenotype was observed solely in the deletion study were for DGCs CdgG and VF_A0476 as well as predicted degenerate protein VF_0355, where Δ*cdgG*, Δ*VF_A0476*, and Δ*VF_0355* strains each yielded the unexpected phenotype of decreased motility and we did not observe any significant cellulose or motility phenotypes upon overexpression of these factors.

The proteins we observed to exhibit the strongest phenotypes were DGCs VF_1200, VF_A0057, VF_A0152, VF_A0155, VF_A0276, VF_A0368, VF_A0567, and VF_A0692; PDEs VF_1603, VF_2480, VF_A0506, and VF_A0551; and dual-function protein VF_0985 (**FIG. 2 and 6**). We also identified interesting phenotypes in VF_0985, which inhibits motility only when magnesium is absent. For all of these proteins, little work has been conducted on a mechanistic basis, and our study presents candidates to pursue that may mediate relevant signaling in the host or during key lifestyle transitions. A benefit of the overexpression approach is that it can reveal phenotypes that are not apparent during single deletions. For example, a protein that is expressed during host colonization or in a specific environmental condition, but not during culture growth, may be assayed for function in this manner. Conversely, a limitation of our method is that the likely higher levels of each examined protein obscures natural regulation that will certainly be relevant to understand signaling *in vivo*. Therefore, this work pares down a complex family of 50 proteins to a narrower set for more focused individual studies.

While the data in **Figure 6** are remarkably consistent, it is clear that there are situations in which protein overexpression impacts motility and not cellulose, or motility in some media and not others. In fact, on a fine scale there are 11 different patterns to the overexpression data among *V. fischeri* proteins in **Figure 6**. This result is even more remarkable given that there was no difference in transcriptional regulation in our experimental setup. Although we detected distinct protein levels that likely suggest posttranscriptional regulation (**FIG. 3**), steady state protein levels did not correlate with the magnitude of the cellulose or motility phenotypes observed.

Therefore, our results suggest that local signaling effects—e.g., localization, protein-protein interactions—may play a major role in how these factors mediate host interactions. The factors that impacted motility in the expected direction (but did not have a significant affect on cellulose production) were DGCs VF_1350, VF_A0342, VF_A0381, and MifB. Conversely, cellulose production (but not motility) was impacted on overexpression of PDEs VF_0087, VF_0091, VF_1367, and VF_A0526. In the case of the DGCs, all four are predicted to have transmembrane domain(s) (54), raising the possibility that membrane localization, and perhaps localization at the flagellar pole may impact the motility-specific phenotype.

The effects of local signaling and protein-protein interactions by c-di-GMP-modulating proteins is particularly exemplified by dual-function proteins as has been demonstrated across Gram-negative bacteria. *Pseudomonas aeruginosa* RmcA encodes GGDEF and EAL domains, both of which are functional, but subcellular localization of RmcA mediated by interaction with the response regulator CbrB activates RmcA PDE activity, subsequently reducing type III secretion system gene expression and increasing biofilm formation (30). *V. cholerae* dual-function protein MbaA interacts with the periplasmic binding protein NspS, which senses norspermidine and activates MbaA DGC activity to increase the local c-di-GMP pool (76, 77). C-di-GMP synthesized by MbaA binds to specific high-affinity biofilm effectors when norspermidine levels are low, sensitizing the cell to norspermidine (77). *Pseudomonas fluorescens* encodes 43 proteins that metabolize c-di-GMP, and when tested across a broad range of conditions it was determined that ligand signaling, protein-protein interactions, and/or transcriptional regulation are all central to c-di-GMP signaling, thus highlighting the importance of local c-di-GMP signaling (78). This backdrop of growing evidence for local signaling and regulated activity of distinct DGCs and PDEs provide hints as to where such regulation could occur in *V. fischeri* given the unique patterns in our data. Recent publication of a more sensitive reporter that is

amenable to single-cell imaging may be a valuable tool to investigate both the levels and subcellular dynamics of c-di-GMP in *V. fischeri* (79).

We previously demonstrated that global *V. fischeri* c-di-GMP levels need to be kept sufficiently low to successfully colonize squid (36), but the specific signals and pathways involved are yet to be determined. During colonization initiation, *V. fischeri* responds to squid-derived signals to help guide them to the light organ (37, 80–83). Therefore it is likely that one or more squid-specific signals may be sensed by c-di-GMP-modulating proteins to elicit effects on certain biofilm and/or motility pathways. Our study presents a set of DGCs and PDEs that are demonstrably functional in multiple assays in *V. fischeri*, and provide strong candidates as proteins to regulate c-di-GMP levels to facilitate functional and reproducible squid host colonization.

MATERIALS AND METHODS

Bacterial strains, plasmids, and media

V. fischeri and *E. coli* strains used in this study are listed in Table 1. Plasmids used in this study are listed in Table 2. *V. fischeri* strains were grown at 25°C in Luria-Bertani salt (LBS) medium (per liter: 25 g Difco LB broth [BD], 10 g NaCl, 50 mM Tris buffer [pH 7.5]) or tryptone broth salt (TBS) medium (per liter: 10 g Bacto Tryptone [Gibco], 20 g NaCl, 35 mM $MgSO_4$ [where noted], 10 mM $CaCl_2$ [where noted], 50 mM Tris buffer [pH 7.5]) where noted. *E. coli* strains used for cloning and conjugation were grown at 37°C in Luria-Bertani (LB) medium (per liter: 25 g Difco LB broth [BD]). When needed, antibiotics were added to the media at the following concentrations: kanamycin, 100 µg/mL for *V. fischeri* and 50 µg/mL for *E. coli*; gentamicin, 2.5 µg/mL for *V. fischeri* and 5 µg/mL for *E. coli*. When needed, 100 µM isopropyl ß-D-1-thiogalactopyranoside (IPTG) was added to the media. For Congo red media, 40 µg/mL Congo

red and 15 µg/mL Coomassie blue were added to LBS. When needed, growth media was solidified using 1.5% agar. Plasmids were introduced from *E. coli* strains into *V. fischeri* strains using standard techniques (84, 85).

DNA synthesis and sequencing

Primers used in this study are listed in Table 3 and were synthesized by Integrated DNA Technologies (Coralville, IA). Gibson primers for all plasmids except pRYI039 and pEVS143-VF_A0506 were designed using the NEBuilder online tool. Site-directed mutagenesis primers were designed using the NEBaseChanger online tool. Full inserts for cloned constructs and active site mutant constructs were confirmed by Sanger Sequencing at Northwestern University Center for Genetic Medicine, ACGT, Inc. (Wheeling, IL), Functional Biosciences (Madison, WI), and/or whole plasmid sequencing by Plasmidsaurus (Eugene, OR). Sequence data were analyzed using DNASTAR or Benchling. PCR to amplify constructs for cloning and sequencing was performed using Pfx50 DNA Polymerase (Invitrogen) or Q5 High-Fidelity DNA polymerase (NEB). Diagnostic PCR was performed using GoTaq polymerase (Promega).

Construction of pRYI039

pEVS143 was amplified using primers RYI354 and RYI355. pRYI039 was assembled by Gibson assembly using the NEBuilder HiFi DNA Assembly Master Mix (NEB). The assembly reaction was transformed into chemically competent NEB5α cells and candidate transformants were selected using kanamycin. The plasmid was screened by PCR using primers M13 -48 rev and MRH049. The plasmid was confirmed by Sanger sequencing using primers M13 -48 rev and MRH049.

Construction of the overexpression plasmids

pEVS143 was amplified using pEVS143_expF and pEVS143_expR primers. Gene ORFs were amplified from MJM1100 genomic DNA using gene-specific forward and reverse primers. Amplified gene inserts were assembled with amplified pEVS143 by Gibson assembly using NEB Gibson Assembly Cloning Kit (NEB) or NEBuilder HiFi DNA Assembly Master Mix (NEB). The assembly reactions were transformed into chemically competent NEB5α or DH5α λpir cells and candidate transformants were selected using kanamycin. Each plasmid was screened by PCR using primers MJM-738F and MJM739R; M13 -48 rev and MJM-739R; or MJM-738F and the respective assembly reverse primer, MJM-739R and the assembly forward primer, and/or MJM-738F and MJM739R. To construct pEVS143-VF_A1014, *VF_A1014* was synthesized with flanking AvrII and BamHI restriction sites and cloned into pEVS143 by GenScript (Piscataway, NJ) and plasmid was confirmed by whole plasmid sequencing. pEVS143-VF_A0506 was confirmed by Sanger sequencing using primers M13 -48 rev, RYI225, RYI226, RYI227, RYI228, RYI229, RYI230, and MRH049. Remaining plasmids were confirmed by Sanger sequencing using primers MJM-738F and MJM-739R; MJM-738F and the respective assembly reverse primer and/or MJM-739R and the assembly forward primer; or pEVS143_seqF and pEVS143_seqR.

Construction of FLAG-tagged protein overexpression plasmids

Plasmids were amplified using site-directed mutagenesis primers to introduce active site mutations. Active site mutant plasmids were assembled using the Q5 Site-Directed Mutagenesis Kit (NEB). Site-directed mutagenesis reactions were transformed into chemically competent DH5α λpir cells and candidate transformants were selected using kanamycin. Each plasmid was screened by PCR using primers M13 -48 rev and MJM-739R and confirmed by whole plasmid sequencing.

Construction of the DGC and PDE active site mutant overexpression plasmids

Plasmids were amplified using site-directed mutagenesis primers to introduce active site mutations. Active site mutant plasmids were assembled using the Q5 Site-Directed Mutagenesis Kit (NEB). Site-directed mutagenesis reactions were transformed into chemically competent NEB5α or DH5α λpir cells and candidate transformants were selected using kanamycin. Each plasmid was screened by PCR using primers M13 -48 rev and MJM739R; or MJM-738F and the respective assembly reverse primer, MJM-739R and the assembly forward primer, and MJM-738F and MJM739R. pEVS143-VF_0989(GAEEF) was confirmed by Sanger sequencing using primers RYI370 and RYI372. pEVS143-VF_A0057(SADEF) was confirmed by Sanger sequencing using primers RYI365 and RYI366. pEVS143-VF_A1038 was confirmed by Sanger sequencing using primers RYI520, RYI521, RYI522, RYI523, MJM-738F, and MJM-739R. Remaining active site mutant plasmids were confirmed by whole plasmid sequencing or Sanger sequencing using primers MJM-738F and MJM-739R; MJM-738F and the respective template plasmid Gibson assembly reverse primer and/or MJM-739R and the template plasmid Gibson assembly forward primer; or pEVS143_seqF and pEVS143_seqR.

Assembly of arrayed strain collections

Strains were streaked on LBS agar and incubated overnight at 25°C. Liquid LBS was inoculated with single colonies of each strain in a deep-well 96-well plate and grown overnight at 23-25°C on a shaker. Overnight cultures were saved in glycerol stocks in 96-well plates in triplicate. For VF_1561, VF_A0152, VF_A0342, and VF_A0551, errors were found in the strains in the wild-type background in the original assays, and the corrected strains were reanalyzed in the same 96-well format in a new arrayed strain collection alongside select additional strains (pRYI039, pEVS143, VF_0087, and VF_0091, VF_0985, and MifA) as controls.

Congo red biofilm assay

Liquid LBS was inoculated with 2 µL of glycerol stock of each strain from an arrayed strain collection and grown at room temperature (23-25°C) overnight on a shaker. 2 µL spots of liquid culture were spotted on LBS Congo red agar and incubated 24 h at 25°C. Spots were transferred onto white printer paper (86) and images were scanned as TIFF or JPEG files. Congo red binding was quantified using ImageJ software (version 2.0.0-rc-69/1.52p) as described in the "Data analysis" section below.

Motility assay

Liquid LBS was inoculated 2 µL of glycerol stock of each strain from an arrayed strain collection and grown at room temperature (23-25°C) overnight on a shaker. 2 µL spots of liquid culture were spotted on TBS, TBS-Mg^{2+} (35 mM $MgSO_4$), and TBS-Ca^{2+} (10 mM $CaCl_2$) agar and incubated overnight at 25°C. The spotted strains were inoculated into TBS, TBS-Mg^{2+}, and TBS-Ca^{2+} soft (0.3%) agar, respectively, using a 96-pin replicator and incubated at 25°C for 3 h for TBS plates and 2.5 h for TBS-Mg^{2+} and TBS-Ca^{2+} plates. Images of plates were taken using a Nikon D810 digital camera and diameter of migration was measured using ImageJ software (version 2.0.0-rc-69/1.52p).

Western blot analysis

One milliliter of overnight culture was pelleted then washed and lysed in 1% SDS solution. To standardize the total protein concentration, the volume of SDS was adjusted based on the Optical Density at 600 nm (OD_{600}). Lysed cells were pelleted to remove cell debris, and the solution was mixed at a 1:1 ratio with 2x Laemmli sample buffer from Bio-Rad (Hercules, CA) to which β-mercaptoethanol had been added. Solution was heated at 95°C for 15 min and loaded onto a 4-20% Mini-Protean TGX Precast Stain Free Gel from Bio-Rad (Hercules, CA). Gel was transferred to a Immun-Blot Low Fluorescence polyvinylidene difluoride (PVDF) membrane and

blocked overnight in 5% nonfat milk resuspended in 1x Tris-buffered saline Tween-20 (1x TBS-T). 2 µL of anti-FLAG Rabbit IgG (800 µG/mL, Sigma-Aldrich) was used as the primary antibody in 0.5% nonfat milk suspended in 1x TBS-T. 2 µL of anti-RpoA Mouse IgG (500 µG/mL, Biolegend) was used as a loading control, binding the RNAP α subunit. 2 µL of LI-COR IRDye 800CW Goat anti-Rabbit IgG (1,000 µg/mL) was used as the secondary antibody, resuspended in 0.5% nonfat milk in 1x TBS-T. 2 µL of LI-COR IRDye 680RD Goat anti-mouse IgG (1,000 µg/mL) was used as the secondary antibody of the loading control. Washes were done with 1x TBS-T, with the final wash being 1x TBS. Blots were analyzed at 700 and 800 nm wavelengths using the LI-COR Odyssey Fc Imager.

C-di-GMP reporter activity quantification

Liquid LBS was inoculated with 5 µL of glycerol stock of each strain from an arrayed strain collection and grown at room temperature (23-25°C) overnight on a shaker. 2 or 4 µL of liquid culture were spotted onto LBS agar and incubated at 25°C for 24 h. For assay of strains not in 96-well format (**FIG. S2B and C**), strains were streaked on LBS agar and single colonies were inoculated into liquid LBS and grown at room temperature (23-25°C) overnight on a shaker. 4 or 8 µL of liquid culture were spotted onto LBS agar and incubated at 25°C for 24 h. For both versions of the assay, spots were resuspended in 500 µL 70% Instant Ocean (IO), then OD_{600}, TurboRFP (555 nm excitation/585 nm emission), and AmCyan (453 nm excitation/486 nm emission) for each resuspended spot were measured in triplicate using BioTek Synergy Neo2 plate reader. To calculate c-di-GMP reporter activity, TurboRFP values (reports on c-di-GMP) were normalized to AmCyan values (constitutively expressed).

ELISA c-di-GMP quantification

Overnight cultures were spotted onto LBS agar and incubated at 25°C overnight. Spots were resuspended in UltraPure water (Cayman Chemical), pelleted in a table top microcentrifuge,

and frozen at -80°C. To standardize cell density, Bacteria Protein Extraction Reagent (B-PER, Thermo Fisher Scientific) was added to cell pellets at a ratio of 1:4 w/v then incubated for 10 min at room temperature (23-25°C). Cell debris was pelleted and the supernatants were diluted for c-di-GMP quantification. Samples were processed and quantified using the Cyclic di-GMP ELISA Kit by Cayman Chemical (Item #501780). Absorbance of the samples were measured at 450 nm using a BioTek Synergy Neo2 plate reader to determine c-di-GMP concentration. A standard curve was generated using the provided Cayman Chemical ELISA Analysis Tool, followed by sample quantification using the standard curve.

Data analysis

Congo red binding was quantified using ImageJ (version 2.0.0-rc-69/1.52p) by subtracting the WT gray value from the mutant gray value and multiplying the value by -1 (36). Fluorescence of reporter strains in liquid culture and ELISA samples were measured using a BioTek Synergy Neo2 plate reader. Western blots were imaged using the LI-COR Odyssey Fc Imager. GraphPad Prism was used to generate graphs and conduct statistical analyses. Graphs were further refined in Adobe Illustrator.

ACKNOWLEDGMENTS

We are grateful to Ella Rotman and John Brooks for early contributions to the project; Ketan Kotla for active site mutant construction; and Chris Waters for the pEVS143-QrgB and pEVS143-VC1086 plasmids. This study was funded by NIGMS grant R35 GM148385 to M.J.M., and R.Y.I. was supported by NIGMS training grant T32 GM007215.

FIGURE LEGENDS

FIG 1. *V. fischeri* encodes 50 proteins across both chromosomes predicted to modulate c-di-GMP levels. The circular chromosomes are represented in a linear fashion for this representation. Numbers represent VF_ locus tags (e.g., VF_0087, VF_A0056, etc.).

FIG 2. Many predicted *V. fischeri* DGCs and PDEs impact biofilm formation and swimming motility when overexpressed. A. Quantification of Congo red binding for *V. fischeri* strains overexpressing the indicated proteins relative to the pRYI039 empty vector control. For each strain, n = 3-8 biological replicates (24 for controls). Congo red images are representative. **B.** Quantification of migration through soft (0.3%) agar for *V. fischeri* strains overexpressing the indicated proteins relative to the pRYI039 empty vector control. For each strain, n = 4-11 biological replicates (33 for controls). For panels A and B, one-way analysis of variance (ANOVA) was used for statistical analysis, each bar represents the means of biological replicates, error bars represent standard errors of the mean, asterisks represent significance relative to the pRYI039 empty vector control (*, $P < 0.05$), numbers represent VF_ locus tags (e.g., VF_0087, VF_A0056, etc.); negative controls pRYI039 and pEVS143 as well as non-*V. fischeri* controls QrgB and VC1086 are also listed and indicated with a black dot.

FIG 3. Most *V. fischeri* proteins tested are expressed from the overexpression vector. Western blot of whole-cell lysates of *V. fischeri* expressing indicated FLAG-tagged proteins from the pEVS143 vector. Predicted band sizes (kD) for each protein are indicated in parentheses. Anti-FLAG Rabbit IgG was used as the primary antibody and LI-COR IRDye 800CW Goat anti-Rabbit IgG was used as the secondary antibody. Anti-RpoA Mouse IgG was used as a loading control, binding the RNAP α subunit, and LI-COR IRDye 680RD Goat anti-mouse IgG was used

as the secondary antibody of the loading control. Western blot is representative of n = 3 biological replicates.

FIG 4. Active site residues are required to modulate cellulose production and motility for selected DGCs and PDEs. A. Quantification of Congo red binding for *V. fischeri* strains overexpressing the indicated proteins relative to the pRYI039 empty vector control. For each strain, n = 4-5 biological replicates (10 for controls). **B.** Quantification of migration through soft (0.3%) agar for V. fischeri strains overexpressing the indicated proteins relative to the pRYI039 empty vector control. For each strain, n = 5 biological replicates (10 for controls). For A and B, unpaired t tests were used for statistical analysis, each bar represents the means of biological replicates, error bars represent standard errors of the mean, asterisks represent significance of a mutant relative to the corresponding wildtype protein (*, $P < 0.01$) and numbers represent VF_ locus tags (e.g., VF_0087, VF_A0056, etc.); negative controls pRYI039 and pEVS143 are indicated with a black dot.

FIG 5. VF_0985 is the only dual-function protein with strong active site-dependent phenotypes. A. Quantification of Congo red binding for *V. fischeri* strains overexpressing the indicated proteins relative to the pRYI039 empty vector control. For each strain, n = 4-5 biological replicates (10 for controls). **B.** Quantification of migration through soft (0.3%) agar for *V. fischeri* strains overexpressing the indicated proteins relative to the pRYI039 empty vector control. For each strain, n = 5 biological replicates (10 for controls). For A and B, unpaired t tests were used for statistical analysis, each bar represents the means of biological replicates, error bars represent standard errors of the mean, asterisks represent significance of a mutant relative to the corresponding wildtype protein (*, $P < 0.05$) and numbers represent VF_ locus tags (e.g., VF_0087, VF_A0056, etc.); negative controls pRYI039 and pEVS143 are indicated with a black dot.

FIG 6. Integration of phenotypic data for the *V. fischeri* DGCs and PDEs. Numbers represent VF_ locus tags (e.g., VF_0087, VF_A0056, etc.); non-*V. fischeri* controls QrgB and VC1086 are also listed. Overexpression data are from this study; deletion data are integrated from Shrestha *et al*., 2022. Blue coloring indicates phenotypes expected from elevated c-di-GMP, whereas pink indicates phenotypes expected from reduced c-di-GMP. White indicates no significant change. [a]This study, [b]Shrestha *et al.* 2022.

FIG S1. Many predicted *V. fischeri* DGCs and PDEs impact swimming motility when overexpressed. A. Summary of motility results for overexpression of indicated proteins in TBS, TBS-Mg, and TBS-Ca soft (0.3%) agar. Blue coloring indicates phenotypes expected from elevated c-di-GMP, whereas pink indicates phenotypes expected from reduced c-di-GMP. White indicates no significant change. **B.** Quantification of migration through TBS, TBS-Mg, and TBS-Ca soft (0.3%) agar for *V. fischeri* strains overexpressing the indicated proteins relative to the pRYI039 empty vector control. TBS data is the same as represented in FIG 2B. For each strain, n = 4-12 biological replicates (33-36 for controls). One-way analysis of variance (ANOVA) was used for statistical analysis, each bar represents the means of biological replicates, error bars represent standard errors of the mean, asterisks represent significance relative to the pRYI039 empty vector control (*, $P < 0.05$), and numbers represent VF_ locus tags (e.g., VF_0087, VF_A0056, etc.); negative controls pRYI039 and pEVS143 as well as non-*V. fischeri* controls QrgB and VC1086 are also listed and indicated with a black dot.

FIG S2. C-di-GMP biosensor activity. Quantification of c-di-GMP concentration for *V. fischeri* strains overexpressing the indicated proteins using the pFY4535 c-di-GMP reporter plasmid. **A.** Assays performed in 96-well format. Values are relative to the pRYI039 empty vector control. For each strain, n = 3-6 (15 for control) biological replicates. **B.** Assays performed in non-96-

well format. Values are relative to the pRYI039 empty vector control. For each strain, n = 3-7 biological replicates (11 for control). **C.** Assays of indicated proteins overexpressed in a high c-di-GMP background. For each strain, n = 3-9 biological replicates. **D.** Integration of phenotypic data for the *V. fischeri* DGCs and PDEs. Blue coloring indicates phenotypes expected from elevated c-di-GMP, whereas pink indicates phenotypes expected from reduced c-di-GMP. White indicates no significant change. For A to C, constitutive AmCyan was used to normalize TurboRFP to cell density, one-way analysis of variance (ANOVA) was used for statistical analysis, each bar represents the means of biological replicates, error bars represent standard errors of the mean, asterisks represent significance relative to the pRYI039 empty vector control (*, $P < 0.02$). For A to D, numbers represent VF_ locus tags (e.g., VF_0087, VF_A0056, etc.); negative controls pRYI039 and pEVS143 as well as non-*V. fischeri* controls QrgB and VC1086 are also listed and indicated with a black dot.

FIG. S3. C-di-GMP quantification methods do not match PDE functional characterization. **A.** Quantification of Congo red binding for *V. fischeri* PDEs overexpressing the indicated proteins relative to the pRYI039 empty vector control. For each strain, n = 5 biological replicates. Each bar represents the means of biological replicates. Data are the same as those represented in FIG 2A. **B.** Quantification of migration through soft (0.3%) agar for *V. fischeri* PDEs overexpressing the indicated proteins relative to the pRYI039 empty vector control. For each strain, n = 4 biological replicates. Each bar represents the means of biological replicates. Data are the same as those represented in FIG 2B. **C.** Quantification of c-di-GMP concentration for *V. fischeri* strains overexpressing the indicated PDEs using the pFY4535 c-di-GMP reporter plasmid (left y-axis; open dots) and ELISA (right y-axis; solid dots). Values are relative to the pRYI039 empty vector control. For each strain, n = 3 (9 for controls) biological replicates, dots represent the means of technical replicates, average bars represent the means of biological replicates. C-di-GMP reporter data are the same as those represented in FIG S2A. For A-C,

error bars represent standard errors of the mean and numbers represent VF_ locus tags (e.g., VF_0087, VF_A0056, etc.); negative control pRYI039 and non-*V. fischeri* control VC1086 are also listed and indicated with a black dot.

Table 1. Strains

Strain	Genotype	Source or Reference(s)
V. fischeri		
MJM1100 = ES114	Natural isolate, squid light-organ (Mandel Lab Stock)	(50, 87)
MJM2775	MJM1100 / pEVS143	(65)
MJM4094	MJM1100 / pRYI039	This study
MJM3822	MJM1100 / pEVS143-QrgB	This study (plasmid from Chris Waters)
MJM3823	MJM1100 / pEVS143-VC1086	This study (plasmid from Chris Waters)
MJM3091	MJM1100 / pEVS143-VF_0087	This study
MJM3092	MJM1100 / pEVS143-VF_0091	This study
MJM3093	MJM1100 / pEVS143-VF_0094	This study
MJM3094	MJM1100 / pEVS143-VF_0355	This study
MJM2766	MJM1100 / pEVS143-VF_0494	This study
MJM2772	MJM1100 / pEVS143-VF_0596	This study
MJM3815	MJM1100 / pEVS143-VF_0985	This study
MJM2773	MJM1100 / pEVS143-VF_0989	This study
MJM3095	MJM1100 / pEVS143-VF_1200	This study
MJM3096	MJM1100 / pEVS143-VF_1245	This study
MJM3097	MJM1100 / pEVS143-VF_1350	This study
MJM3098	MJM1100 / pEVS143-VF_1367	This study
MJM3099	MJM1100 / pEVS143-VF_1515	This study
MJM6214	MJM1100 / pEVS143-VF_1561	This study
MJM3820	MJM1100 / pEVS143-VF_1603	This study

MJM3100	MJM1100 / pEVS143-VF_1639	This study
MJM3932	MJM1100 / pEVS143-VF_2261	This study
MJM3101	MJM1100 / pEVS143-VF_2362	This study
MJM3821	MJM1100 / pEVS143-VF_2480	This study
MJM2767	MJM1100 / pEVS143-VF_A0056	This study
MJM3102	MJM1100 / pEVS143-VF_A0057	This study
MJM2769	MJM1100 / pEVS143-VF_A0152	This study
MJM3103	MJM1100 / pEVS143-VF_A0155	This study
MJM3816	MJM1100 / pEVS143-VF_A0216	This study
MJM3818	MJM1100 / pEVS143-VF_A0244	This study
MJM2770	MJM1100 / pEVS143-VF_A0276	This study
MJM3104	MJM1100 / pEVS143-VF_A0323	This study
MJM6213	MJM1100 / pEVS143-VF_A0342	This study
MJM3106	MJM1100 / pEVS143-VF_A0343	This study
MJM3814	MJM1100 / pEVS143-VF_A0344	This study
MJM3824	MJM1100 / pEVS143-VF_A0344	This study
MJM3933	MJM1100 / pEVS143-VF_A0368	This study
MJM2768	MJM1100 / pEVS143-VF_A0368	This study
MJM3107	MJM1100 / pEVS143-VF_A0381	This study
MJM3108	MJM1100 / pEVS143-VF_A0398	This study
MJM3109	MJM1100 / pEVS143-VF_A0475	This study
MJM3817	MJM1100 / pEVS143-VF_A0476	This study
MJM3110	MJM1100 / pEVS143-VF_A0526	This study
MJM6215	MJM1100 / pEVS143-VF_A0551	This study
MJM3112	MJM1100 / pEVS143-VF_A0567	This study
MJM3113	MJM1100 / pEVS143-VF_A0692	This study
MJM3114	MJM1100 / pEVS143-VF_A0706	This study
MJM3115	MJM1100 / pEVS143-VF_A0796	This study

MJM3116	MJM1100 / pEVS143-VF_A0879	This study
MJM3117	MJM1100 / pEVS143-VF_A0959	This study
MJM3819	MJM1100 / pEVS143-VF_A0976	This study
MJM2771	MJM1100 / pEVS143-VF_A1012	This study
MJM2765	MJM1100 / pEVS143-VF_A1038	This study
MJM3118	MJM1100 / pEVS143-VF_A1076	This study
MJM3119	MJM1100 / pEVS143-VF_A1166	This study
MJM4289	MJM1100 / pEVS143-VF_0989-FLAG	This study
MJM4291	MJM1100 / pEVS143-VF_A0155-FLAG	This study
MJM4293	MJM1100 / pEVS143-VF_A0057-FLAG	This study
MJM6170	MJM1100 / pEVS143-VF_A0056-FLAG	This study
MJM6171	MJM1100 / pEVS143-VF_1515-FLAG	This study
MJM6193	MJM1100 / pEVS143-VF_A0476-FLAG	This study
MJM6216	MJM1100 / pEVS143-VF_A0342-FLAG	This study
MJM6220	MJM1100 / pEVS143-VF_A0216-FLAG	This study
MJM5574	MJM1100 / pEVS143-VF_0091(GAAEF, AAL)	This study
MJM5573	MJM1100 / pEVS143-VF_0091(GAAEF)	This study
MJM5263	MJM1100 / pEVS143-VF_0094(AAL, GADEF)	This study
MJM5095	MJM1100 / pEVS143-VF_0094(AAL)	This study
MJM5096	MJM1100 / pEVS143-VF_0094(GADEF)	This study
MJM5099	MJM1100 / pEVS143-VF_0596(SAEEF)	This study
MJM4092	MJM1100 / pEVS143-VF_0989(GAEEF)	This study
MJM4084	MJM1100 / pEVS143-VF_A0057(SADEF)	This study
MJM5572	MJM1100 / pEVS143-VF_A0152(GADEF)	This study
MJM5256	MJM1100 / pEVS143-VF_A0244(AAL, GADEF)	This study
MJM5097	MJM1100 / pEVS143-VF_A0244(AAL)	This study
MJM5254	MJM1100 / pEVS143-VF_A0244(GADEF)	This study
MJM5255	MJM1100 / pEVS143-VF_A0475(AAL)	This study

MJM5098	MJM1100 / pEVS143-VF_A0475(GADEF)	This study
MJM5100	MJM1100 / pEVS143-VF_A0796(GAEEF)	This study
MJM5354	MJM1100 / pEVS143-VF_A0976(GADEF)	This study
MJM4296	MJM1100 / pEVS143-VF_A1038(AAL)	This study
MJM4106	MJM1100 / pRYI039;pFY4535	This study
MJM4821	MJM1100 / pEVS143-QrgB;pFY4535	This study
MJM4971	MJM1100 / pEVS143-VC1086;pFY4535	This study
MJM4767	MJM1100 / pEVS143-VF_0087;pFY4535	This study
MJM4793	MJM1100 / pEVS143-VF_0091;pFY4535	This study
MJM4794	MJM1100 / pEVS143-VF_0094;pFY4535	This study
MJM4795	MJM1100 / pEVS143-VF_0355;pFY4536	This study
MJM4686	MJM1100 / pEVS143-VF_0494; pFY4535	This study
MJM4791	MJM1100 / pEVS143-VF_0596;pFY4535	This study
MJM4689	MJM1100 / pEVS143-VF_0985; pFY4535	This study
MJM4024	MJM1100 / pEVS143-VF_0989;pFY4535	This study
MJM4796	MJM1100 / pEVS143-VF_1200;pFY4535	This study
MJM4797	MJM1100 / pEVS143-VF_1245;pFY4535	This study
MJM4798	MJM1100 / pEVS143-VF_1350;pFY4535	This study
MJM4687	MJM1100 / pEVS143-VF_1367; pFY4535	This study
MJM4799	MJM1100 / pEVS143-VF_1515;pFY4535	This study
MJM6218	MJM1100 / pEVS143-VF_1561;pFY4535	This study
MJM4769	MJM1100 / pEVS143-VF_1603;pFY4535	This study
MJM4768	MJM1100 / pEVS143-VF_1639;pFY4535	This study
MJM4770	MJM1100 / pEVS143-VF_2261;pFY4535	This study
MJM4800	MJM1100 / pEVS143-VF_2362;pFY4535	This study
MJM4820	MJM1100 / pEVS143-VF_2480;pFY4535	This study
MJM4787	MJM1100 / pEVS143-VF_A0056;pFY4535	This study
MJM4108	MJM1100 / pEVS143-VF_A0057;pFY4535	This study

MJM4788	MJM1100 / pEVS143-VF_A0152;pFY4535	This study
MJM4110	MJM1100 / pEVS143-VF_A0155;pFY4535	This study
MJM4816	MJM1100 / pEVS143-VF_A0216;pFY4535	This study
MJM4818	MJM1100 / pEVS143-VF_A0244;pFY4535	This study
MJM4789	MJM1100 / pEVS143-VF_A0276;pFY4535	This study
MJM4801	MJM1100 / pEVS143-VF_A0323;pFY4535	This study
MJM6217	MJM1100 / pEVS143-VF_A0342;pFY4535	This study
MJM4803	MJM1100 / pEVS143-VF_A0343;pFY4536	This study
MJM4815	MJM1100 / pEVS143-VF_A0344;pFY4535	This study
MJM4822	MJM1100 / pEVS143-VF_A0368;pFY4535	This study
MJM4804	MJM1100 / pEVS143-VF_A0381;pFY4535	This study
MJM4688	MJM1100 / pEVS143-VF_A0398; pFY4535	This study
MJM4805	MJM1100 / pEVS143-VF_A0475;pFY4535	This study
MJM4817	MJM1100 / pEVS143-VF_A0476;pFY4535	This study
MJM4823	MJM1100 / pEVS143-VF_A0506;pFY4535	This study
MJM4806	MJM1100 / pEVS143-VF_A0526;pFY4535	This study
MJM6219	MJM1100 / pEVS143-VF_A0551;pFY4535	This study
MJM4808	MJM1100 / pEVS143-VF_A0567;pFY4535	This study
MJM4809	MJM1100 / pEVS143-VF_A0692;pFY4535	This study
MJM4203	MJM1100 / pEVS143-VF_A0706; pFY4535	This study
MJM4810	MJM1100 / pEVS143-VF_A0796;pFY4535	This study
MJM4811	MJM1100 / pEVS143-VF_A0879;pFY4535	This study
MJM4812	MJM1100 / pEVS143-VF_A0959;pFY4535	This study
MJM4819	MJM1100 / pEVS143-VF_A0976;pFY4535	This study
MJM4790	MJM1100 / pEVS143-VF_A1012;pFY4535	This study
MJM4023	MJM1100 / pEVS143-VF_A1038;pFY4535	This study
MJM4813	MJM1100 / pEVS143-VF_A1076;pFY4535	This study
MJM4814	MJM1100 / pEVS143-VF_A1166;pFY4535	This study

MJM5576	MJM1100 / pFY4535;pEVS143-VF_0091(GAAEF)	This study
MJM5659	MJM1100 / pFY4535;pEVS143-VF_0091(AAL)	This study
MJM5637	MJM1100 / pFY4535;pEVS143-VF_0091(GAAEF,AAL)	This study
MJM5638	MJM1100 / pFY4535;pEVS143-VF_0094(GADEF)	This study
MJM5639	MJM1100 / pFY4535;pEVS143-VF_0094(AAL)	This study
MJM5640	MJM1100 / pFY4535;pEVS143-VF_0094(GADEF,AAL)	This study
MJM5226	MJM1100 / pEVS143-VF_0094(AAL);pFY4535	This study
MJM5227	MJM1100 / pEVS143-VF_0094(GADEF);pFY4535	This study
MJM4969	MJM1100 / pEVS143-0494(AAL);pFY4535	This study
MJM4970	MJM1100 / pEVS143-0494(GADEF);pFY4535	This study
MJM5645	MJM1100 / pFY4535;pEVS143-VF_0494(AAL,GADEF)	This study
MJM5641	MJM1100 / pFY4535;pEVS143-VF_0596(SAEEF)	This study
MJM5642	MJM1100 / pFY4535;pEVS143-VF_0985(GADEF)	This study
MJM5643	MJM1100 / pFY4535;pEVS143-VF_0985(AVL)	This study
MJM5644	MJM1100 / pFY4535;pEVS143-VF_0985(GADEF,AVL)	This study
MJM4107	MJM1100 / pEVS143-VF_0989(GAEEF);pFY4535	This study
MJM5648	MJM1100 / pFY4535;pEVS143-VF_1639(GAEEF)	This study
MJM4109	MJM1100 / pEVS143-VF_A0057(SADEF);pFY4535	This study
MJM5575	MJM1100 / pFY4535;pEVS143-VF_A0152(GADEF)	This study
MJM5655	MJM1100 / pFY4535;pEVS143-VF_A0244(AAL)	This study
MJM5646	MJM1100 / pFY4535;pEVS143-VF_A0244(GADEF)	This study
MJM5656	MJM1100 / pFY4535;pEVS143-VF_A0244(AAL, GADEF)	This study
MJM5647	MJM1100 / pFY4535;pEVS143-VF_A0344(AVL)	This study
MJM5650	MJM1100 / pFY4535;pEVS143-VF_A0475(AAL)	This study
MJM5649	MJM1100 / pFY4535;pEVS143-VF_A0475(GADEF)	This study
MJM5651	MJM1100 / pFY4535;pEVS143-VF_A0475(AAL,GADEF)	This study
MJM5654	MJM1100 / pFY4535;pEVS143-VF_A0796(GAEEF)	This study
MJM5652	MJM1100 / pFY4535;pEVS143-VF_A0976(GADEF)	This study

MJM5653	MJM1100 / pFY4535;pEVS143-VF_A1038(AAL)	This study
MJM4106	Δ6PDE / pRYI039;pFY4535	This study
MJM5861	Δ6PDE / pVF_0087;pFY4535	This study
MJM5884	Δ6PDE / pVF_0091;pFY4535	This study
MJM5862	Δ6PDE / pVF_0494;pFY4535	This study
MJM4399	Δ6PDE / pVF_1367;pFY4535	This study
MJM4400	Δ6PDE / pVF_1603;pFY4535	This study
MJM4401	Δ6PDE / pVF_2480;pFY4535	This study
MJM5863	Δ6PDE / pVF_A0216;pFY4535	This study
MJM5864	Δ6PDE / pVF_A0244;pFY4535	This study
MJM4202	Δ6PDE / pVF_A0506;pFY4535	This study
MJM4204	Δ6PDE / pVF_A0706;pFY4535	This study
MJM5885	Δ6PDE / pVF_A1014;pFY4535	This study
MJM4205	Δ6PDE / pVF_A1038;pFY4535	This study
MJM5866	Δ6PDE / pVF_A1076;pFY4535	This study
MJM5867	Δ6PDE / pVF_A1166;pFY4535	This study
MJM4403	Δ6PDE / pVC1086;pFY4535	This study
E. coli		
MJM534	CC118 λpir / pEVS104	*(84)*
MJM2466	DH5α λpir / pEVS143	*(65)*
MJM3999	NEB5α / pFY4535	*(71)*
MJM4064	NEB5α / pEVS143-ΔGFP-CmR	This study
MJM2470	DH5α λpir / pEVS143-VC1086	This study (plasmid from Chris Waters)
MJM2468	DH5α λpir / pEVS143-QrgB	This study (plasmid from Chris Waters)
MJM2524	NEB5α / pEVS143-VF_0087	This study
MJM2521	NEB5α / pEVS143-VF_0091	This study
MJM2811	NEB5α / pEVS143-VF_0094	This study

MJM2516	NEB5α / pEVS143-VF_0355	This study
MJM2500	NEB5α / pEVS143-VF_0494	This study
MJM2506	NEB5α / pEVS143-VF_0596	This study
MJM2525	NEB5α / pEVS143-VF_0985	This study
MJM2507	NEB5α / pEVS143-VF_0989	This study
MJM2526	NEB5α / pEVS143-VF_1200	This study
MJM2807	NEB5α / pEVS143-VF_1245	This study
MJM2522	NEB5α / pEVS143-VF_1350	This study
MJM2518	NEB5α / pEVS143-VF_1367	This study
MJM2527	NEB5α / pEVS143-VF_1515	This study
MJM6201	NEB5α / pEVS143-VF_1561	This study
MJM3089	NEB5α / pEVS143-VF_1603	This study
MJM2509	NEB5α / pEVS143-VF_1639	This study
MJM2528	NEB5α / pEVS143-VF_2261	This study
MJM2515	NEB5α / pEVS143-VF_2362	This study
MJM2815	NEB5α / pEVS143-VF_2432	This study
MJM3090	NEB5α / pEVS143-VF_2480	This study
MJM2501	NEB5α / pEVS143-VF_A0056	This study
MJM2519	NEB5α / pEVS143-VF_A0057	This study
MJM2503	NEB5α / pEVS143-VF_A0152	This study
MJM2802	NEB5α / pEVS143-VF_A0155	This study
MJM2803	NEB5α / pEVS143-VF_A0216	This study
MJM2806	NEB5α / pEVS143-VF_A0244	This study
MJM2504	NEB5α / pEVS143-VF_A0276	This study
MJM2809	NEB5α / pEVS143-VF_A0323	This study
MJM6200	NEB5α / pEVS143-VF_A0342	This study
MJM2512	NEB5α / pEVS143-VF_A0343	This study
MJM2520	NEB5α / pEVS143-VF_A0344	This study

MJM2502	NEB5α / pEVS143-VF_A0368	This study
MJM2513	NEB5α / pEVS143-VF_A0381	This study
MJM2805	NEB5α / pEVS143-VF_A0398	This study
MJM2523	NEB5α / pEVS143-VF_A0475	This study
MJM2804	NEB5α / pEVS143-VF_A0476	This study
MJM3982	DH5α λpir / pEVS143-VF_A0506	This study
MJM2810	NEB5α / pEVS143-VF_A0526	This study
MJM6202	NEB5α / pEVS143-VF_A0551	This study
MJM2510	NEB5α / pEVS143-VF_A0567	This study
MJM2517	NEB5α / pEVS143-VF_A0692	This study
MJM2529	NEB5α / pEVS143-VF_A0706	This study
MJM2511	NEB5α / pEVS143-VF_A0796	This study
MJM2813	NEB5α / pEVS143-VF_A0879	This study
MJM2808	NEB5α / pEVS143-VF_A0959	This study
MJM2812	NEB5α / pEVS143-VF_A0976	This study
MJM2505	NEB5α / pEVS143-VF_A1012	This study
MJM4907	DH5α λpir / pEVS143-VF_A1014	This study
MJM2499	NEB5α / pEVS143-VF_A1038	This study
MJM2814	NEB5α / pEVS143-VF_A1076	This study
MJM2801	NEB5α / pEVS143-VF_A1166	This study
MJM4280	DH5α λpir / pEVS143-VF_0989-FLAG	This study
MJM4282	DH5α λpir / pEVS143-VF_A0155-FLAG	This Study
MJM4284	DH5α λpir / pEVS143-VF_A0057-FLAG	This study
MJM6158	DH5α λpir / pEVS143-VF_A0056-FLAG	This study
MJM6159	DH5α λpir / pEVS143-VF_1515-FLAG	This study
MJM6191	DH5α λpir / pEVS143-VF_A0216-FLAG	This study
MJM6192	DH5α λpir / pEVS143-VF_A0476-FLAG	This study
MJM6204	DH5α λpir / pEVS143-VF_A0342-FLAG	This study

MJM4921	DH5α λpir / pEVS143-VF_0087(ACL)	This study
MJM5307	NEB5α / pEVS143-VF_0091(AAL)	This study
MJM5551	NEB5α / pEVS143-VF_0091(GAAEF, AAL)	This study
MJM5550	NEB5α / pEVS143-VF_0091(GAAEF)	This study
MJM5248	DH5α λpir / pEVS143-VF_0094(AAL, GADEF)	This study
MJM5038	DH5α λpir / pEVS143-VF_0094(AAL)	This study
MJM5039	DH5α λpir / pEVS143-VF_0094(GADEF)	This study
MJM4922	DH5α λpir / pEVS143-VF_0494(AAL)	This study
MJM4923	DH5α λpir / pEVS143-VF_0494(GADEF)	This study
MJM5042	DH5α λpir / pEVS143-VF_0596(SAEEF)	This study
MJM4935	DH5α λpir / pEVS143-VF_0985(AVL)	This study
MJM5499	NEB5α / pEVS143-VF_0985(GADEF, AVL)	This study
MJM4974	DH5α λpir / pEVS143-VF_0985(GADEF)	This study
MJM4065	NEB5α / pEVS143-VF_0989(GAEEF)	This study
MJM4287	NEB5α / pEVS143-VF_1038(AAL)	This study
MJM4936	DH5α λpir / pEVS143-VF_1367(HAIGK)	This study
MJM3179	NEB5α / pEVS143-VF_1639(GAEEF)	This study
MJM4070	NEB5α / pEVS143-VF_A0057(SADEF)	This study
MJM3180	NEB5α / pEVS143-VF_A0152(GADEF)	This study
MJM5249	DH5α λpir / pEVS143-VF_A0244(AAL, GADEF)	This study
MJM5040	DH5α λpir / pEVS143-VF_A0244(AAL)	This study
MJM5093	DH5α λpir / pEVS143-VF_A0244(GADEF)	This study
MJM5301	NEB5α / pEVS143-VF_A0344(AVL)	This study
MJM4924	DH5α λpir / pEVS143-VF_A0398(GADEF)	This study
MJM5232	DH5α λpir / pEVS143-VF_A0475(AAL, GADEF)	This study
MJM5094	DH5α λpir / pEVS143-VF_A0475(AAL)	This study
MJM5041	DH5α λpir / pEVS143-VF_A0475(GADEF)	This study
MJM5043	DH5α λpir / pEVS143-VF_A0796(GAEEF)	This study

734
735 **Table 2. Plasmids**
736

Plasmid	Description	Source or Reference(s)
pEVS104	Conjugal helper plasmid (Kan^R)	(84)
pEVS143	IPTG-inducible overexpression vector (Kan^R)	(65)
pRYI039	Empty vector control for pEVS143 constructs; pEVS143-Δ*gfp-cmR* (Kan^R)	This study
pEVS143-VC1086	pEVS143 carrying *VC1086* (Kan^R)	(59)
pEVS143-QrgB	pEVS143 carrying *QrgB* (Kan^R)	(59)
pEVS143-VF_0087	pEVS143 carrying *VF_0087* (Kan^R)	This study
pEVS143-VF_0091	pEVS143 carrying *VF_0091* (Kan^R)	This study
pEVS143-VF_0094	pEVS143 carrying *VF_0094* (Kan^R)	This study
pEVS143-VF_0355	pEVS143 carrying *VF_0355* (Kan^R)	This study
pEVS143-VF_0494	pEVS143 carrying *VF_0494* (Kan^R)	This study
pEVS143-VF_0596	pEVS143 carrying *VF_0596* (Kan^R)	This study
pEVS143-VF_0985	pEVS143 carrying *VF_0985* (Kan^R)	This study
pEVS143-VF_0989	pEVS143 carrying *VF_0989* (*mifA*) (Kan^R)	This study
pEVS143-VF_1200	pEVS143 carrying *VF_1200* (Kan^R)	This study
pEVS143-VF_1245	pEVS143 carrying *VF_1245* (Kan^R)	This study

pEVS143-VF_1350	pEVS143 carrying *VF_1350* (Kan^R)	This study
pEVS143-VF_1367	pEVS143 carrying *VF_1367* (Kan^R)	This study
pEVS143-VF_1515	pEVS143 carrying *VF_1515* (Kan^R)	This study
pEVS143-VF_1561	pEVS143 carrying *VF_1561* (Kan^R)	This study
pEVS143-VF_1603	pEVS143 carrying *VF_1603* (Kan^R)	This study
pEVS143-VF_1639	pEVS143 carrying *VF_1639* (*casA*) (Kan^R)	This study
pEVS143-VF_2261	pEVS143 carrying *VF_2261* (Kan^R)	This study
pEVS143-VF_2362	pEVS143 carrying *VF_2362* (Kan^R)	This study
pEVS143-VF_2432	pEVS143 carrying *VF_2432* (Kan^R)	This study
pEVS143-VF_2480	pEVS143 carrying *VF_2480* (Kan^R)	This study
pEVS143-VF_A0056	pEVS143 carrying *VF_A0056* (Kan^R)	This study
pEVS143-VF_A0057	pEVS143 carrying *VF_A0057* (Kan^R)	This study
pEVS143-VF_A0152	pEVS143 carrying *VF_A0152* (Kan^R)	This study
pEVS143-VF_A0155	pEVS143 carrying *VF_A0155* (Kan^R)	This study
pEVS143-VF_A0216	pEVS143 carrying *VF_A0216* (Kan^R)	This study
pEVS143-VF_A0244	pEVS143 carrying *VF_A0244* (Kan^R)	This study
pEVS143-VF_A0276	pEVS143 carrying *VF_A0276* (Kan^R)	This study

pEVS143-VF_A0323	pEVS143 carrying *VF_A0323* (Kan^R)	This study
pEVS143-VF_A0342	pEVS143 carrying *VF_A0342* (Kan^R)	This study
pEVS143-VF_A0343	pEVS143 carrying *VF_A0343* (Kan^R)	This study
pEVS143-VF_A0344	pEVS143 carrying *VF_A0344* (Kan^R)	This study
pEVS143-VF_A0368	pEVS143 carrying *VF_A0368* (Kan^R)	This study
pEVS143-VF_A0381	pEVS143 carrying *VF_A0381* (Kan^R)	This study
pEVS143-VF_A0398	pEVS143 carrying *VF_A0398* (Kan^R)	This study
pEVS143-VF_A0475	pEVS143 carrying *VF_A0475* (Kan^R)	This study
pEVS143-VF_A0476	pEVS143 carrying *VF_A0476* (Kan^R)	This study
pEVS143-VF_A0506	pEVS143 carrying *VF_A0506* (Kan^R)	This study
pEVS143-VF_A0526	pEVS143 carrying *VF_A0526* (Kan^R)	This study
pEVS143-VF_A0551	pEVS143 carrying *VF_A0551* (Kan^R)	This study
pEVS143-VF_A0567	pEVS143 carrying *VF_A0567* (Kan^R)	This study
pEVS143-VF_A0692	pEVS143 carrying *VF_A0692* (Kan^R)	This study
pEVS143-VF_A0706	pEVS143 carrying *VF_A0706* (Kan^R)	This study
pEVS143-VF_A0796	pEVS143 carrying *VF_0796* (Kan^R)	This study
pEVS143-VF_A0879	pEVS143 carrying *VF_A0879* (Kan^R)	This study

pEVS143-VF_A0959	pEVS143 carrying *VF_A0959* (*mifB*) (Kan^R)	This study
pEVS143-VF_A0976	pEVS143 carrying *VF_A0976* (Kan^R)	This study
pEVS143-VF_A1012	pEVS143 carrying *VF_A1012* (Kan^R)	This study
pEVS143-A1014	pEVS143 carrying *VF_A1014* (*pdeV*) (Kan^R)	This study
pEVS143-VF_A1038	pEVS143 carrying *VF_A1038* (*binA*) (Kan^R)	This study
pEVS143-VF_A1076	pEVS143 carrying *VF_A1076* (Kan^R)	This study
pEVS143-VF_A1166	pEVS143 carrying *VF_A1166* (*lapD*) (Kan^R)	This study
pEVS143-VF_0989-FLAG	pEVS143 carrying *VF_0989-FLAG* (*mifA*) (Kan^R)	This study
pEVS143-VF_A0155-FLAG	pEVS143 carrying *VF_A0155-FLAG* (Kan^R)	This study
pEVS143-VF_A0057-FLAG	pEVS143 carrying *VF_A0057-FLAG* (Kan^R)	This study
pEVS143-VF_1515-FLAG	pEVS143 carrying *VF_1515-FLAG* (Kan^R)	This study
pEVS143-VF_A0056-FLAG	pEVS143 carrying *VF_A0056-FLAG* (Kan^R)	This study
pEVS143-VF_A0216-FLAG	pEVS143 carrying *VF_A0216-FLAG* (Kan^R)	This study
pEVS143-VF_A0342-FLAG	pEVS143 carrying *VF_A0342-FLAG* (Kan^R)	This study
pEVS143-VF_A0476-FLAG	pEVS143 carrying *VF_A0476-FLAG* (Kan^R)	This study
pEVS143-VF_0087(ACL)	pEVS143 carrying *VF_0087* with ACL active site mutation (Kan^R)	This study
pEVS143-VF_0091(AAL)	pEVS143 carrying *VF_0091* with AAL active site mutation (Kan^R)	This study

pEVS143-VF_0091(GAAEF, AAL)	pEVS143 carrying *VF_0091* with GAAEF and AAL active site mutations (Kan^R)	This study
pEVS143-VF_0091(GAAEF)	pEVS143 carrying *VF_0091* with GAAEF active site mutation (Kan^R)	This study
pEVS143-VF_0094(AAL, GADEF)	pEVS143 carrying *VF_0094* with AAL and GADEF active site mutations (Kan^R)	This study
pEVS143-VF_0094(AAL)	pEVS143 carrying *VF_0094* with AAL active site mutation (Kan^R)	This study
pEVS143-VF_0094(GADEF)	pEVS143 carrying *VF_0094* with GADEF active site mutation (Kan^R)	This study
pEVS143-VF_0494(AAL)	pEVS143 carrying *VF_0494* with AAL active site mutation (Kan^R)	This study
pEVS143-VF_0494(GADEF)	pEVS143 carrying *VF_0494* with GADEF active site mutation (Kan^R)	This study
pEVS143-VF_0596(SAEEF)	pEVS143 carrying *VF_0596* with SAEEF active site mutation (Kan^R)	This study
pEVS143-VF_0985(AVL)	pEVS143 carrying *VF_0985* with AVL active site mutation (Kan^R)	This study
pEVS143-VF_0985(GADEF, AVL)	pEVS143 carrying *VF_0985* with GADEF and AVL active site mutations (Kan^R)	This study
pEVS143-VF_0985(GADEF)	pEVS143 carrying *VF_0985* with GADEF active site mutation (Kan^R)	This study
pEVS143-MifA(GAEEF)	pEVS143 carrying *VF_0989* (*mifA*) with GAEEF active site mutation (Kan^R)	This study
pEVS143-VF_1367(HAIGK)	pEVS143 carrying *VF_1367* with HAIGK active site mutation (Kan^R)	This study
pEVS143-VF_CasA(GAEEF)	pEVS143 carrying *VF_1639* (*casA*) with GAEEF active site mutation (Kan^R)	This study
pEVS143-VF_A0057(SADEF)	pEVS143 carrying *VF_A0057* with SADEF active site mutation (Kan^R)	This study
pEVS143-VF_A0152(GADEF)	pEVS143 carrying *VF_A0152* with GADEF active site mutation (Kan^R)	This study
pEVS143-VF_A0244(AAL, GADEF)	pEVS143 carrying *VF_A0244* with AAL and GADEF active site mutations (Kan^R)	This study

pEVS143-VF_A0244(AAL)	pEVS143 carrying *VF_A0244* with AAL active site mutation (Kan^R)	This study
pEVS143-VF_A0244(GADEF)	pEVS143 carrying *VF_A0244* with GADEF active site mutation (Kan^R)	This study
pEVS143-VF_A0344(AVL)	pEVS143 carrying *VF_A0344* with AVL active site mutation (Kan^R)	This study
pEVS143-VF_A0398(GADEF)	pEVS143 carrying *VF_A0398* with GADEF active site mutation (Kan^R)	This study
pEVS143-VF_A0475(AAL, GADEF)	pEVS143 carrying *VF_A0475* with AAL and GADEF active site mutations (Kan^R)	This study
pEVS143-VF_A0475(AAL)	pEVS143 carrying *VF_A0475* with AAL active site mutation (Kan^R)	This study
pEVS143-VF_A0475(GADEF)	pEVS143 carrying *VF_A0475* with GADEF active site mutation (Kan^R)	This study
pEVS143-VF_A0796(GAEEF)	pEVS143 carrying *VF_A0796* with GAEEF active site mutation (Kan^R)	This study
pEVS143-BinA(AAL)	pEVS143 carrying *VF_A1038* (*binA*) with AAL active site mutation (Kan^R)	This study
pFY4535	c-di-GMP reporter plasmid ($Gent^R$)	(71)

Table 3. Primers

Primer name	**Sequence (5'-3')**	**Notes**
RYI354	GGAAGCTAAAGATCCGGTGAttgattgagcaa	Forward primer to amplify pEVS143 without *gfp* and c*mR* cassettes for Gibson assembly of pRYI039
RYI355	TCACCGGATCTTTAGCTTCCttagctccctgaattc	Reverse primer to amplify pEVS143 without *gfp* and c*mR* cassettes for Gibson assembly of pRYI039
pEVS143_expF	GATCCGGTGATTGATTGAGCAA	Forward primer to amplify pEVS143 excluding *gfp* and *cmR* for Gibson assembly to insert ORF of gene of interest
pEVS143_expR	TTTAGCTTCCTTAGCTCCTGAATTC	Reverse primer to amplify pEVS143 excluding *gfp* and *cmR* for Gibson assembly to insert ORF of gene of interest
0087_F	gagctaaggaagctaaaATGCAAACTCTCTCATTTAGTG	Forward primer to amplify *VF_0087* for Gibson assembly into pEVS143

0087_R	caatcaatcaccggatcTTACGTCTTAATG TGTAACGATTTAG	Reverse primer to amplify *VF_0087* for Gibson assembly into pEVS143
0091_F	gagctaaggaagctaaaATGACAGTGGTA CTTAACAGCC	Forward primer to amplify *VF_0091* for Gibson assembly into pEVS143
0091_R	caatcaatcaccggatcTCACGCCTGAGA ACGATGAATC	Reverse primer to amplify *VF_0091* for Gibson assembly into pEVS143
0094_F	gagctaaggaagctaaaATGACAGAACCA ACACATAAAAAAC	Forward primer to amplify *VF_0094* for Gibson assembly into pEVS143
0094_R	caatcaatcaccggatcTTATTCTGTTGGC CAATCTTCTAAAG	Reverse primer to amplify *VF_0094* for Gibson assembly into pEVS143
0355_F	gagctaaggaagctaaaATGAGAAAAACG CCTAGTTTAC	Forward primer to amplify *VF_0355* for Gibson assembly into pEVS143
0355_R	caatcaatcaccggatcTTATTTACCCCAA CGGCTTCTTC	Reverse primer to amplify *VF_0355* for Gibson assembly into pEVS143
0494_F	gagctaaggaagctaaaATGTCTCTTTCT CAAATACAACATTG	Forward primer to amplify *VF_0494* for Gibson assembly into pEVS143
0494_R	caatcaatcaccggatcTTATCTAGCGCGT TTGTTTTGTAC	Reverse primer to amplify *VF_0494* for Gibson assembly into pEVS143
0596_F	gagctaaggaagctaaaATGATTGAAGTA TCCATTGTTGCC	Forward primer to amplify *VF_0596* for Gibson assembly into pEVS143
0596_R	caatcaatcaccggatcCTACGCACTAAT GAGTTGCTCAATG	Reverse primer to amplify *VF_0596* for Gibson assembly into pEVS143
0985_F	gagctaaggaagctaaaATGCTGCATAAG TCTGATAAAAG	Forward primer to amplify *VF_0985* for Gibson assembly into pEVS143
0985_R	caatcaatcaccggatcTTATGCATATTTT GCTTTTAATTCAC	Reverse primer to amplify *VF_0985* for Gibson assembly into pEVS143
0989_F	gagctaaggaagctaaaATGAATCTCAAG CAAATAAAATATTTTATC	Forward primer to amplify *VF_0989* (*mifA*) for Gibson assembly into pEVS143
0989_R	caatcaatcaccggatcTCATGCGATTTGA TCCATTTCAC	Reverse primer to amplify *VF_0989* (*mifA*) for Gibson assembly into pEVS143
1200_F	gagctaaggaagctaaaATGGCTAAGAAT CAATGGAATG	Forward primer to amplify *VF_1200* for Gibson assembly into pEVS143
1200_R	caatcaatcaccggatcTTAATACATGGTT TCTTTGATATGC	Reverse primer to amplify *VF_1200* for Gibson assembly into pEVS143
1245_F	gagctaaggaagctaaaATGCCTCAATCT CGTCTTCAGC	Forward primer to amplify *VF_1245* for Gibson assembly into pEVS143
1245_R	caatcaatcaccggatcTTATATATCTTGA TAGTGAGTGATTTTATTACGC	Reverse primer to amplify *VF_1245* for Gibson assembly into pEVS143
1350_F	gagctaaggaagctaaaATGAACCTTAGG CTTTTAACAG	Forward primer to amplify *VF_1350* for Gibson assembly into pEVS143
1350_R	caatcaatcaccggatcTTAAATATCATAA AAGTGATTGCTCTG	Reverse primer to amplify *VF_1350* for Gibson assembly into pEVS143

1367_F	gagctaaggaagctaaaATGTGTGTTTTTTCTTCATTTGTTTC	Forward primer to amplify *VF_1367* for Gibson assembly into pEVS143
1367_R	caatcaatcaccggatcTTACTGATTATTCTCAAAAATAGCTC	Reverse primer to amplify *VF_1367* for Gibson assembly into pEVS143
1515_F	gagctaaggaagctaaaATGAGGTTCGTTTATCTATCCG	Forward primer to amplify *VF_1515* for Gibson assembly into pEVS143
1515_R	caatcaatcaccggatcTCAGCCTCGAATGGTAACTTGA	Reverse primer to amplify *VF_1515* for Gibson assembly into pEVS143
1561_F	gagctaaggaagctaaaATGAGCATTTTTCAAAAAATTGC	Forward primer to amplify *VF_1561* for Gibson assembly into pEVS143
1561_R	caatcaatcaccggatcTTAATTCATATAATGTATATTTGAACTTGAG	Reverse primer to amplify *VF_1561* for Gibson assembly into pEVS143
1603_F	gagctaaggaagctaaaATGTACACATATGTTGCTCGTC	Forward primer to amplify *VF_1603* for Gibson assembly into pEVS143
1603_R	aatcaatcaccggatcCTATTTTGCTATCTCATCTACCC	Reverse primer to amplify *VF_1603* for Gibson assembly into pEVS143
1639_F	gagctaaggaagctaaaATGCCGAAATTTAATTTAAAACATATC	Forward primer to amplify *VF_1639* (*casA*) for Gibson assembly into pEVS143
1639_R	caatcaatcaccggatcTTATGAAAAGTAAACTCGGTTTTTAC	Reverse primer to amplify *VF_1639* (*casA*) for Gibson assembly into pEVS143
2261_F	gagctaaggaagctaaaATGCATTATAAAAAAACGAAAGC	Forward primer to amplify *VF_2261* for Gibson assembly into pEVS143
2261_R	caatcaatcaccggatcCTATGCTAAGTCCTCTAAACTAG	Reverse primer to amplify *VF_2261* for Gibson assembly into pEVS143
2326_F	gagctaaggaagctaaaATGATCTACATGGATGTTTATATG	Forward primer to amplify *VF_2326* for Gibson assembly into pEVS143
2326_R	caatcaatcaccggatcTTATGATTTATCAATTTTCTCTTGGTAC	Reverse primer to amplify *VF_2326* for Gibson assembly into pEVS143
2480_F	gagctaaggaagctaaaATGTATGCATACGTTGCCAGAC	Forward primer to amplify *VF_2480* for Gibson assembly into pEVS143
2480_R	aatcaatcaccggatcCTATTTAGACAAAATACTCTGATACCAC	Reverse primer to amplify *VF_2480* for Gibson assembly into pEVS143
A0056_F	gagctaaggaagctaaaATGTTTCGGTGTTGTATGAGTG	Forward primer to amplify *VF_A0056* for Gibson assembly into pEVS143
A0056_R	caatcaatcaccggatcTCAATCCGTTTCTCGTTTAAGC	Reverse primer to amplify *VF_A0056* for Gibson assembly into pEVS143
A0057_F	gagctaaggaagctaaaATGATACTTCAATGGTTCAGTG	Forward primer to amplify *VF_A0057* for Gibson assembly into pEVS143
A0057_R	caatcaatcaccggatcTTAAACGAGAAACGGATTGATTTC	Reverse primer to amplify *VF_A0057* for Gibson assembly into pEVS143
A0152_F	gagctaaggaagctaaaATGAGGGTAAAAAATATCGTTG	Forward primer to amplify *VF_A0152* for Gibson assembly into pEVS143

A0152_R	caatcaatcaccggatcTTACTCAGATATAAAAACTTGGTTTC	Reverse primer to amplify *VF_A0152* for Gibson assembly into pEVS143
A0155_F	gagctaaggaagctaaaATGAAAAATCGAAGTGCTTTTTTTTATAG	Forward primer to amplify *VF_A0155* for Gibson assembly into pEVS143
A0155_R	caatcaatcaccggatcTTACAATTCAAACCTAACACAG	Reverse primer to amplify *VF_A0155* for Gibson assembly into pEVS143
A0216_F	gagctaaggaagctaaaATGAAAAGTAAAATAAATATAATATTAGTAGATGATATTG	Forward primer to amplify *VF_A0216* for Gibson assembly into pEVS143
A0216_R	caatcaataccggatcTTAACATTGAAGGTTTTCAGTTTC	Reverse primer to amplify *VF_A0216* for Gibson assembly into pEVS143
A0244_F	gagctaaggaagctaaaATGATTATGAATAAATACTTCATTTATCAGCC	Forward primer to amplify *VF_A0244* for Gibson assembly into pEVS143
A0244_R	caatcaatcaccggatcTCATGCTGGGTGAAGCTTATTTTTC	Reverse primer to amplify *VF_A0244* for Gibson assembly into pEVS143
A0276_F	gagctaaggaagctaaaATGAAACCAATCCATATAGACTC	Forward primer to amplify *VF_A0276* for Gibson assembly into pEVS143
A0276_R	caatcaatcaccggatcTTAATCCTCAGGTGAAACAATTTG	Reverse primer to amplify *VF_A0276* for Gibson assembly into pEVS143
A0323_F	gagctaaggaagctaaaATGATCATGACAAATAAGAAAATGC	Forward primer to amplify *VF_A0323* for Gibson assembly into pEVS143
A0323_R	caatcaatcaccggatcTTATATAGAATCAGAGCACTTTTTTG	Reverse primer to amplify *VF_A0323* for Gibson assembly into pEVS143
CSH043	caggagctaaggaagctaaaATGTTTAATGTTAAATTATTTGGATTAGATAAGCTTTTCTT	Forward primer to amplify *VF_A0342* for Gibson assembly into pEVS143
CSH044	gctcaatcaatcaccggatcCTAAAAATCATAATTGTTCTTATCTAATGTAACTATGTTACGG	Reverse primer to amplify *VF_A0342* for Gibson assembly into pEVS143
A0343_F	gagctaaggaagctaaaATGATTTTTAGCAATGTTGATAATAATAATATG	Forward primer to amplify *VF_A0343* for Gibson assembly into pEVS143
A0343_R	caatcaatcaccggatcTTATCCTTCAAATACCGTTACTTTG	Reverse primer to amplify *VF_A0343* for Gibson assembly into pEVS143
A0344_F	gagctaaggaagctaaaATGAAATTTATTACTAATAAATATATTGTTTATTTGTTG	Forward primer to amplify *VF_A0344* for Gibson assembly into pEVS143
A0344_R	caatcaatcaccggatcTTAATCACGCATTATGGAATGAAAATTATC	Reverse primer to amplify *VF_A0344* for Gibson assembly into pEVS143
A0368_F	gagctaaggaagctaaaATGAAAAAATTAATCTTGCTGCTTG	Forward primer to amplify *VF_A0368* for Gibson assembly into pEVS143
A0368_R	caatcaatcaccggatcTTAATAGATACTGTCGTTCAAAATAAC	Reverse primer to amplify *VF_A0368* for Gibson assembly into pEVS143
A0381_F	gagctaaggaagctaaaATGGATGGCATAATCCAACTCTC	Forward primer to amplify *VF_A0381* for Gibson assembly into pEVS143

A0381_R	caatcaatcaccggatcTTATTCGCTGACG CAGTTACGT	Reverse primer to amplify *VF_A0381* for Gibson assembly into pEVS143
A0398_F	gagctaaggaagctaaaATGGACAGTCTT TTAAATCGAATAG	Forward primer to amplify *VF_A0398* for Gibson assembly into pEVS143
A0398_R	caatcaatcaccggatcTTAATAAGAACAT ACTTTATTCTTTCCG	Reverse primer to amplify *VF_A0398* for Gibson assembly into pEVS143
A0475_F	gagctaaggaagctaaaTTGAATTCAACA ATTTCTTTCTTATATC	Forward primer to amplify *VF_A0475* for Gibson assembly into pEVS143
A0475_R	caatcaatcaccggatcTCACTGTAATTTT CTGCTTTTG	Reverse primer to amplify *VF_A0475* for Gibson assembly into pEVS143
A0476_F	gagctaaggaagctaaaATGCTATCGTTT ATTTATATGAGTG	Forward primer to amplify *VF_A0476* for Gibson assembly into pEVS143
A0476_R	caatcaatcaccggatcTTATACTTTATTT CTATTTTTATATTGAAACTTTG	Reverse primer to amplify *VF_A0476* for Gibson assembly into pEVS143
A0506_F	caggagctaaggaagctaaaATGCGTCATT ACCTATCTCTAG	Forward primer to amplify *VF_A0506* for Gibson assembly into pEVS143
A0506_R	gctcaatcaatcaccggatcTTAATCGGGAT ATTCAAGTCGAATATC	Reverse primer to amplify *VF_A0506* for Gibson assembly into pEVS143
A0526_F	gagctaaggaagctaaaATGAGATTAATT GAAGCAAAACTG	Forward primer to amplify *VF_A0526* for Gibson assembly into pEVS143
A0526_R	caatcaatcaccggatcTCAATAATAATTC TTTTTAAAATTTGAAATTGTATTTTT ATAATTAAC	Reverse primer to amplify *VF_A0526* for Gibson assembly into pEVS143
A0551_F	gagctaaggaagctaaaATGCTATTGGCA ACACAGGACG	Forward primer to amplify *VF_A0551* for Gibson assembly into pEVS143
A0551_R	caatcaatcaccggatcTTAAGCCGCTTG ATGATTTTGTTC	Reverse primer to amplify *VF_A0551* for Gibson assembly into pEVS143
A0567_F	gagctaaggaagctaaaATGAAGTGGATA GAAAATGCATC	Forward primer to amplify *VF_A0567* for Gibson assembly into pEVS143
A0567_R	caatcaatcaccggatcTCAAATTTTGTGA AACATATACTTTC	Reverse primer to amplify *VF_A0567* for Gibson assembly into pEVS143
A0692_F	gagctaaggaagctaaaATGACGATGCTA AGACGATTAATG	Forward primer to amplify *VF_A0692* for Gibson assembly into pEVS143
A0692R	caatcaatcaccggatcTCAATTTGCCATA GTGACACGG	Reverse primer to amplify *VF_A0692* for Gibson assembly into pEVS143
A0706_F	gagctaaggaagctaaaGTGTTTAAACGT AAGAATTCGC	Forward primer to amplify *VF_A0706* for Gibson assembly into pEVS143
A0706_R	caatcaatcaccggatcTTATTTATTACGA TTGGTATCAATCTG	Reverse primer to amplify *VF_A0706* for Gibson assembly into pEVS143
A0796_F	gagctaaggaagctaaaATGAATTCTGAT ATGAGTGATTTTCATTG	Forward primer to amplify *VF_A0796* for Gibson assembly into pEVS143
A0796_R	caatcaatcaccggatcTTATGGCATTAAG GTGGTGCAA	Reverse primer to amplify *VF_A0796* for Gibson assembly into pEVS143

A0879_F	gagctaaggaagctaaaATGCCTACTTATACGTTCAAAAAC	Forward primer to amplify *VF_A0879* for Gibson assembly into pEVS143
A0879_R	caatcaatcaccggatcTCAGAACGCTGATAATGCATCAC	Reverse primer to amplify *VF_A0879* for Gibson assembly into pEVS143
A0959_F	gagctaaggaagctaaaATGATTTCTCGCCCATATGTGAG	Forward primer to amplify *VF_A0959* (*mifB*) for Gibson assembly into pEVS143
A0959_R	caatcaatcaccggatcTTACTGCTGATAATAAGCTTTTTTCTC	Reverse primer to amplify *VF_A0959* (*mifB*) for Gibson assembly into pEVS143
A0976_F	gagctaaggaagctaaaGTGATTACATTTGGTAAGTCCAATAAATTATTTTTTTG	Forward primer to amplify *VF_A0976* for Gibson assembly into pEVS143
A0976_R	caatcaatcaccggatcTCATAGCTTTTCAAATACTTTAAATCC	Reverse primer to amplify *VF_A0976* for Gibson assembly into pEVS143
A1012_F	gagctaaggaagctaaaATGTTAACTGACCAAAAAATTTTAATTG	Forward primer to amplify *VF_A1012* for Gibson assembly into pEVS143
A1012_R	caatcaatcaccggatcTCAAATGGTTATTGTTGATACAC	Reverse primer to amplify *VF_A1012* for Gibson assembly into pEVS143
A1038_F	gagctaaggaagctaaaATGCAAAAAACGTTAACGTCTG	Forward primer to amplify *VF_A1038* (*binA*) for Gibson assembly into pEVS143
A1038_R	caatcaatcaccggatcTTACACAAAGTGAAAGTAGGGG	Reverse primer to amplify *VF_A1038* (*binA*) for Gibson assembly into pEVS143
A1076_F	gagctaaggaagctaaaATGTTCTCAATTAAGAAATTGGTTAATTTTATG	Forward primer to amplify *VF_A1076* for Gibson assembly into pEVS143
A1076_R	caatcaatcaccggatcTTAAGGAATAAGTAGCGGTCTTC	Reverse primer to amplify *VF_A1076* for Gibson assembly into pEVS143
A1166_F	gagctaaggaagctaaaATGACATTATATAAACAACTAGTAGC	Forward primer to amplify *VF_A1166* (*lapD*) for Gibson assembly into pEVS143
A1166_R	caatcaatcaccggatcTTAAATGCCTTCCACTTTTTCATTAATAAAG	Reverse primer to amplify *VF_A1166* (*lapD*) for Gibson assembly into pEVS143
CSH025	gatgatgataaaTAAGATCCGGTGATT	Forward primer to amplify pEVS143-A0216 for site-directed mutagenesis to introduce C-terminal FLAG tag
CSH026	atctttataatcACATTGAAGGTTTTCAG	Reverse primer to amplify pEVS143-A0216 for site-directed mutagenesis to introduce C-terminal FLAG tag
CSH027	gatgatgataaaTAGGATCCGGTGATTG	Forward primer to amplify pEVS143-A0342 for site-directed mutagenesis to introduce C-terminal FLAG tag
CSH028	atctttataatcAAAATCATAATTGTTCTTATC	Reverse primer to amplify pEVS143-A0342 for site-directed mutagenesis to introduce C-terminal FLAG tag
CSH029	gatgatgataaaTAAGATCCGGTGAT	Forward primer to amplify pEVS143-A0476 for site-directed mutagenesis to introduce C-terminal FLAG tag

CSH030	atctttataatcTACTTTATTTCTATTTTTATATTGAAACT	Reverse primer to amplify pEVS143-A0476 for site-directed mutagenesis to introduce C-terminal FLAG tag
CSH033	gatgatgataaaTGAGATCCGGTGATTG	Forward primer to amplify pEVS143-1515 for site-directed mutagenesis to introduce C-terminal FLAG tag
CSH034	atctttataatcGCCTCGAATGGTAAC	Reverse primer to amplify pEVS143-1515 for site-directed mutagenesis to introduce C-terminal FLAG tag
CSH035	gatgatgataaaTGAGATCCGGTGATTG	Forward primer to amplify pEVS143-A0056 for site-directed mutagenesis to introduce C-terminal FLAG tag
CSH036	atctttataatcATCCGTTTCTCGTTTAAG	Reverse primer to amplify pEVS143-A0056 for site-directed mutagenesis to introduce C-terminal FLAG tag
RYI497	gatgatgataaaTGAGATCCGGTGATTGATTG	Forward primer to amplify pEVS143-0989 for site-directed mutagenesis to introduce C-terminal FLAG tag
RYI498	atctttataatcTGCGATTTGATCCATTTC	Reverse primer to amplify pEVS143-0989 for site-directed mutagenesis to introduce C-terminal FLAG tag
RYI499	gatgatgataaaTAAGATCCGGTGATTGATTG	Forward primer to amplify pEVS143-A0155 for site-directed mutagenesis to introduce C-terminal FLAG tag
RYI500	atctttataatcCAATTCAAACCTAACACAG	Reverse primer to amplify pEVS143-A0155 for site-directed mutagenesis to introduce C-terminal FLAG tag
RYI501	gatgatgataaaTAAGATCCGGTGATTGATTG	Forward primer to amplify pEVS143-A0057 for site-directed mutagenesis to introduce C-terminal FLAG tag
RYI502	atctttataatcAACGAGAAACGGATTGATTTC	Reverse primer to amplify pEVS143-A0057 for site-directed mutagenesis to introduce C-terminal FLAG tag
A0152_mutF	TCGCTTGGGCGcTGACGAGTTTG	Forward primer to amplify pEVS143-A0152 for site-directed mutagenesis to introduce GADEF active site change
A0152_mutR	GCGAAATGATCAGATTCACAG	Reverse primer to amplify pEVS143-A0152 for site-directed mutagenesis to introduce GADEF active site change
0087(ACL)_F_V2	AGCATCAACAgcaTGTCTAATGCG	Forward primer to amplify pEVS143-0087 for site-directed mutagenesis to introduce ACL active site change
0087(ACL)_R_V2	AGCTCATGAGTATGCGCTTTATAAATAGGT	Reverse primer to amplify pEVS143-0087 for site-directed mutagenesis to introduce ACL active site change
0091(GAAEF)_F	CGCATTGGTGcaGCTGAGTTTG	Forward primer to amplify pEVS143-0091

		for site-directed mutagenesis to introduce GAAEF active site change
0091(GAAEF)_R	GGCCATTTCTATATTTTGATC	Reverse primer to amplify pEVS143-0091 for site-directed mutagenesis to introduce GAAEF active site change
0091(AAL)_F	CATGGTGCAGcAGCGTTAATTC	Forward primer to amplify pEVS143-0091 for site-directed mutagenesis to introduce AAL active site change
0091(AAL)_R	AATTTTACCGTCTTCAAAATTC	Reverse primer to amplify pEVS143-0091 for site-directed mutagenesis to introduce AAL active site change
0094(AAL)_F	ATCGGTGCGGcAGCATTAATTC	Forward primer to amplify pEVS143-0094 for site-directed mutagenesis to introduce AAL active site change
0094(AAL)_R	GGTTTTTCCACTCTTTATATCAATTATTG	Reverse primer to amplify pEVS143-0094 for site-directed mutagenesis to introduce AAL active site change
0094(GADEF)_F	CGAGTTGGTGcaGATGAATTCGC	Forward primer to amplify pEVS143-0094 for site-directed mutagenesis to introduce GADEF active site change
0094(GADEF)_R	AGCAATGGCAATGTTGTC	Reverse primer to amplify pEVS143-0094 for site-directed mutagenesis to introduce GADEF active site change
0494(AAL)_F	TAATGGCGCAgcaGCCCTTGTTC	Forward primer to amplify pEVS143-0494 for site-directed mutagenesis to introduce AAL active site change
0494(AAL)_R_V2	ATTCTAAAATCACGAGCACTTACTTTTGGTTGGTAC	Reverse primer to amplify pEVS143-0494 for site-directed mutagenesis to introduce AAL active site change
0494(GADEF)_F	CCATTTAGGTgcaGATGAATTTGGAATACTATTTC	Forward primer to amplify pEVS143-0494 for site-directed mutagenesis to introduce GADEF active site change
0494(GADEF)_R	CCAACAACAGCGTGTTTTG	Reverse primer to amplify pEVS143-0494 for site-directed mutagenesis to introduce GADEF active site change
0596(SAEEF)_F	CGTTTTAGTGcaGAAGAATTTTTAATTTTATTTAC	Forward primer to amplify pEVS143-0596 for site-directed mutagenesis to introduce SAEEF active site change
0596(SAEEF)_R	AGCAACAAAATTAGTATCTG	Reverse primer to amplify pEVS143-0596 for site-directed mutagenesis to introduce SAEEF active site change
0985(AVL)_F_V2	TTATGGTGTAgcaGTGCTTTCTCG	Forward primer to amplify pEVS143-0985 for site-directed mutagenesis to introduce AVL active site change
0985(AVL)_R_V2	ATCTCACCTGTTTTAGTATC	Reverse primer to amplify pEVS143-0985 for site-directed mutagenesis to introduce

		AVL active site change
0985(GADEF)_F	ACGTTTTGGCgcaGATGAATTTG	Forward primer to amplify pEVS143-0985 for site-directed mutagenesis to introduce GADEF active site change
0985(GADEF)_R	GCAACTATTTCATCTTTTTCAATAAAG	Reverse primer to amplify pEVS143-0985 for site-directed mutagenesis to introduce GADEF active site change
1367(HAIGK)_F	TTCGCTGCATgcaATTGGAAAGATTG	Forward primer to amplify pEVS143-1367 for site-directed mutagenesis to introduce HAIGK active site change
1367(HAIGK)_R	GCAATCATACGAATTTCTTC	Reverse primer to amplify pEVS143-1367 for site-directed mutagenesis to introduce HAIGK active site change
A0057(SADEF)_F	TCGTCTATCTgcaGATGAGTTTTTACTTGG	Forward primer to amplify pEVS143-A0057 for site-directed mutagenesis to introduce SADEF active site change
A0057(SADEF)_R	GCGACAAGATCGTTTTCAAAAAC	Reverse primer to amplify pEVS143-A0057 for site-directed mutagenesis to introduce SADEF active site change
A0244(GADEF)_F	CGTTTTGGTGcAGATGAGTTTATTTTATG	Forward primer to amplify pEVS143-A0244 for site-directed mutagenesis to introduce GADEF active site change
A0244(GADEF)_R	AATTAATAAATCTTCTTTTCTTAAGTATTTATTAATTAAAC	Reverse primer to amplify pEVS143-A0244 for site-directed mutagenesis to introduce GADEF active site change
A0244(AAL)_F	GTTTCTTACGcAGCATTAATTAGATTTAAAG	Forward primer to amplify pEVS143-A0244 for site-directed mutagenesis to introduce AAL active site change
A0244(AAL)_R	AATAGAACCTTCAAAGAAGTTAG	Reverse primer to amplify pEVS143-A0244 for site-directed mutagenesis to introduce AAL active site change
A0344(AVL)_F	ATTGGAGGGGcaGTATTAGCTC	Forward primer to amplify pEVS143-A0344 for site-directed mutagenesis to introduce AVL active site change
A0344(AVL)_R	GATATTTTCATTAGCATCAACAATAG	Reverse primer to amplify pEVS143-A0344 for site-directed mutagenesis to introduce AVL active site change
A0398(GAEEF)_F	ACGTTATGGAgcaGAAGAGTTTC	Forward primer to amplify pEVS143-A0398 for site-directed mutagenesis to introduce GAEEF active site change
A0398(GAEEF)_R	AGTGTATAGTGAGAAGGTG	Reverse primer to amplify pEVS143-A0398 for site-directed mutagenesis to introduce GAEEF active site change
A0475(AAL)_F	ATCAGTGTTGcAGCTTTACTAAG	Forward primer to amplify pEVS143-A0475 for site-directed mutagenesis to introduce AAL active site change

A0475(AAL)_R	AATACTTCCATTCTGTACTTTTG	Reverse primer to amplify pEVS143-A0475 for site-directed mutagenesis to introduce AAL active site change
A0475(GADEF)_F	AGATACGGTGcaGATGAATTTTTGATTTTTAC	Forward primer to amplify pEVS143-A0475 for site-directed mutagenesis to introduce GADEF active site change
A0475(GADEF)_R	TATGATAAGGTCTTCCTTTC	Reverse primer to amplify pEVS143-A0475 for site-directed mutagenesis to introduce GADEF active site change
A0796(GAEEF)_F	CGATATGGTGcaGAAGAGTTTACC	Forward primer to amplify pEVS143-A0796 for site-directed mutagenesis to introduce GAEEF active site change
A0796(GAEEF)_R	CCCACAAATATCTGTGTTAC	Reverse primer to amplify pEVS143-A0796 for site-directed mutagenesis to introduce GAEEF active site change
A0976(GADEF)_F	CGATTAGGTGcaGATGAATTTGCC	Forward primer to amplify pEVS143-A0976 for site-directed mutagenesis to introduce GADEF active site change
A0976(GADEF)_R	AGCGACGTAACTATTTTC	Reverse primer to amplify pEVS143-A0976 for site-directed mutagenesis to introduce GADEF active site change
BinA(AAL)_F	ATTGGTTGTgcaGCGCTATTAC	Forward primer to amplify pEVS143-BinA for site-directed mutagenesis to introduce AAL active site change
BinA(AAL)_R	CCATTTTTTATTTACTGGGC	Reverse primer to amplify pEVS143-BinA for site-directed mutagenesis to introduce AAL active site change
MifA(GAEEF)_F	AAGAATTGGCgcaGAAGAGTTTG	Forward primer to amplify pEVS143-MifA for site-directed mutagenesis to introduce GAEEF active site change
MifA(GAEEF)_R	GCTACAAAATCAATACTTCG	Reverse primer to amplify pEVS143-MifA for site-directed mutagenesis to introduce GAEEF active site change
pEVS143_seqF	GCACTCCCGTTCTGGATA	Forward primer to amplify gene inserts in pEVS143
pEVS143_seqR	GTATGAGTCAGCAACACC	Reverse primer to amplify gene inserts in pEVS143
MJM-738_F	ACAATTTCACACAGGAAACAGCTC	Forward primer to amplify gene inserts in pEVS143
MJM-739_R	AGCCAGTAATCGAATTGGCTAGTA	Reverse primer to amplify gene inserts in pEVS143
M13 -48 rev	AGCGGATAACAATTTCACACAGG	Forward primer to amplify gene inserts in pEVS143
MRH049	AGGAAAGTCTACACGAACCCT	Reverse primer to amplify gene inserts in pEVS143

RYI231	ATGCGTCATTACCTATCTCTAGTTTGTG	Sequencing primer for *VF_A0506*
RYI232	TGATACCTACAGCAACGATAGGTAGC	Sequencing primer for *VF_A0506*
RYI233	GCTACCTATCGTTGCTGTAGGTATCA	Sequencing primer for *VF_A0506*
RYI234	CGATAGCTTCAGTGTTATCCAAGGAAAG	Sequencing primer for *VF_A0506*
RYI235	GGGATCATCGTTACTCAGTACATTGC	Sequencing primer for *VF_A0506*
RYI236	GGCAAGTTAACACCAGAAGAAAGAACT	Sequencing primer for *VF_A0506*
RYI365	GATGGGTTAACACAATTAGCTAACCGT	Sequencing primer for *VF_A0057*
RYI366	TTAAACGAGAAACGGATTGATTTCTTTTGC	Sequencing primer for *VF_A0057*
RYI370	CAGAGTTGGGAAGGTGAAGTTGTT	Sequencing primer for *mifA*
RYI372	TCATGCGATTTGATCCATTTCACTGG	Sequencing primer for *mifA*
RYI520	TGATCGCCTATTGTGGGTTACCTC	Sequencing primer for *binA*
RYI521	ACTTTTGCATATACATTTTGCTAATAGCCGT	Sequencing primer for *binA*
RYI522	AGTCGTCATTATCTGAACACAAAATTGAACG	Sequencing primer for *binA*
RYI523	GTGGCTTAATTTCTGATGAACCGCT	Sequencing primer for *binA*

740

741

REFERENCES

1. Hooper LV. 2009. Do symbiotic bacteria subvert host immunity? Nat Rev Microbiol 7:367–374.

2. McFall-Ngai M, Nyholm SV, Castillo MG. 2010. The role of the immune system in the initiation and persistence of the *Euprymna scolopes–Vibrio fischeri* symbiosis. Semin Immunol 22:48–53.

3. Alteri CJ, Mobley HLT. 2012. Escherichia coli physiology and metabolism dictates adaptation to diverse host microenvironments. Curr Opin Microbiol 15:3–9.

4. Bliven KA, Maurelli AT. 2016. Evolution of Bacterial Pathogens Within the Human Host. Microbiol Spectr 4:10.1128/microbiolspec.vmbf-0017-2015.

5. Flint A, Butcher J, Stintzi A. 2016. Stress Responses, Adaptation, and Virulence of Bacterial Pathogens During Host Gastrointestinal Colonization. Microbiol Spectr 4:10.1128/microbiolspec.vmbf-0007-2015.

6. Petrova OE, Sauer K. 2012. Sticky situations: key components that control bacterial surface attachment. J Bacteriol 194:2413–2425.

7. Heindl JE, Wang Y, Heckel BC, Mohari B, Feirer N, Fuqua C. 2014. Mechanisms and regulation of surface interactions and biofilm formation in *Agrobacterium*. Front Plant Sci 5:176.

8. Petrova OE, Sauer K. 2016. Escaping the biofilm in more than one way: desorption, detachment or dispersion. Curr Opin Microbiol 30:67–78.

9. Sadiq FA, Flint S, Li Y, Liu T, Lei Y, Sakandar HA, He G. 2017. New mechanistic insights into the motile-to-sessile switch in various bacteria with particular emphasis on *Bacillus*

subtilis and *Pseudomonas aeruginosa*: a review. Biofouling 33:306–326.

10. Berne C, Ellison CK, Ducret A, Brun YV. 2018. Bacterial adhesion at the single-cell level. Nat Rev Microbiol 16:616–627.

11. Valentini M, Gonzalez D, Mavridou DA, Filloux A. 2018. Lifestyle transitions and adaptive pathogenesis of *Pseudomonas aeruginosa*. Curr Opin Microbiol 41:15–20.

12. Raina J-B, Fernandez V, Lambert B, Stocker R, Seymour JR. 2019. The role of microbial motility and chemotaxis in symbiosis. Nat Rev Microbiol 17:284–294.

13. Colin R, Ni B, Laganenka L, Sourjik V. 2021. Multiple functions of flagellar motility and chemotaxis in bacterial physiology. FEMS Microbiol Rev 45:6 fuab038.

14. Zhou B, Szymanski CM, Baylink A. 2023. Bacterial chemotaxis in human diseases. Trends Microbiol 31:453–467.

15. Chambers JR, Sauer K. 2013. Small RNAs and their role in biofilm formation. Trends Microbiol 21:39–49.

16. Esquivel RN, Pohlschroder M. 2014. A conserved type IV pilin signal peptide H-domain is critical for the post-translational regulation of flagella-dependent motility. Mol Microbiol 93:494–504.

17. Kim EA, Blair DF. 2015. Function of the Histone-Like Protein H-NS in Motility of *Escherichia coli*: Multiple Regulatory Roles Rather than Direct Action at the Flagellar Motor. J Bacteriol 197:3110–3120.

18. Yoon SH, Waters CM. 2021. The ever-expanding world of bacterial cyclic oligonucleotide second messengers. Curr Opin Microbiol 60:96–103.

19. Hengge R, Gründling A, Jenal U, Ryan R, Yildiz F. 2016. Bacterial signal transduction by cyclic Di-GMP and other nucleotide second messengers. J Bacteriol 198:15–26.

20. Römling U, Galperin MY, Gomelsky M. 2013. Cyclic di-GMP: the first 25 years of a universal bacterial second messenger. Microbiol Mol Biol Rev 77:1–52.

21. Ross P, Weinhouse H, Aloni Y, Michaeli D, Weinberger-Ohana P, Mayer R, Braun S, de Vroom E, van der Marel GA, van Boom JH, Benziman M. 1987. Regulation of cellulose synthesis in *Acetobacter xylinum* by cyclic diguanylic acid. Nature 325:279–281.

22. Aravind L, Koonin EV. 1998. The HD domain defines a new superfamily of metal-dependent phosphohydrolases. Trends Biochem Sci 23:469–472.

23. Galperin MY, Natale DA, Aravind L, Koonin EV. 1999. A specialized version of the HD hydrolase domain implicated in signal transduction. J Mol Microbiol Biotechnol 1:303–305.

24. Simm R, Morr M, Kader A, Nimtz M, Römling U. 2004. GGDEF and EAL domains inversely regulate cyclic di-GMP levels and transition from sessility to motility. Mol Microbiol 53:1123–1134.

25. Ryan RP, Fouhy Y, Lucey JF, Crossman LC, Spiro S, He Y-W, Zhang L-H, Heeb S, Camara M, Williams P, Maxwell Dow J. 2006. Cell-cell signaling in *Xanthomonas campestris* involves an HD-GYP domain protein that functions in cyclic di-GMP turnover. Proc Natl Acad Sci 103:6712–6717.

26. Sultan SZ, Pitzer JE, Boquoi T, Hobbs G, Miller MR, Motaleb MA. 2011. Analysis of the HD-GYP domain cyclic dimeric GMP phosphodiesterase reveals a role in motility and the enzootic life cycle of *Borrelia burgdorferi*. Infect Immun 79:3273–3283.

27. Christen M, Christen B, Folcher M, Schauerte A, Jenal U. 2005. Identification and

807 Characterization of a Cyclic di-GMP-specific Phosphodiesterase and Its Allosteric Control
808 by GTP*. J Biol Chem 280:30829–30837.

809 28. Feirer N, Xu J, Allen KD, Koestler BJ, Bruger EL, Waters CM, White RH, Fuqua C. 2015. A
810 Pterin-Dependent Signaling Pathway Regulates a Dual-Function Diguanylate Cyclase-
811 Phosphodiesterase Controlling Surface Attachment in *Agrobacterium tumefaciens*. MBio
812 6:e00156.

813 29. Cruz-Pérez JF, Lara-Oueilhe R, Marcos-Jiménez C, Cuatlayotl-Olarte R, Xiqui-Vázquez
814 ML, Reyes-Carmona SR, Baca BE, Ramírez-Mata A. 2021. Expression and function of the
815 *cdgD* gene, encoding a CHASE-PAS-DGC-EAL domain protein, in *Azospirillum brasilense*.
816 Sci Rep 11:520.

817 30. Kong W, Luo W, Wang Y, Liu Y, Tian Q, Zhao C, Liang H. 2022. Dual GGDEF/EAL-Domain
818 Protein RmcA Controls the Type III Secretion System of *Pseudomonas aeruginosa* by
819 Interaction with CbrB. ACS Infect Dis 8:2441–2450.

820 31. Viruega-Góngora VI, Acatitla-Jácome IS, Zamorano-Sánchez D, Reyes-Carmona SR,
821 Xiqui-Vázquez ML, Baca BE, Ramírez-Mata A. 2022. The GGDEF-EAL protein CdgB from
822 *Azospirillum baldaniorum* Sp245, is a dual function enzyme with potential polar localization.
823 PLoS One 17:e0278036.

824 32. Galperin MY, Nikolskaya AN, Koonin EV. 2001. Novel domains of the prokaryotic two-
825 component signal transduction systems. FEMS Microbiol Lett 203:11–21.

826 33. Hall CL, Lee VT. 2018. Cyclic-di-GMP regulation of virulence in bacterial pathogens. Wiley
827 Interdiscip Rev RNA 9:e1454.

828 34. Valentini M, Filloux A. 2019. Multiple Roles of c-di-GMP Signaling in Bacterial
829 Pathogenesis. Annu Rev Microbiol 73:387–406.

35. Robinson CD, Sweeney EG, Ngo J, Ma E, Perkins A, Smith TJ, Fernandez NL, Waters CM, Remington SJ, Bohannan BJM, Guillemin K. 2021. Host-emitted amino acid cues regulate bacterial chemokinesis to enhance colonization. Cell Host Microbe 29:1221–1234.e8.

36. Isenberg RY, Christensen DG, Visick KL, Mandel MJ. 2022. High Levels of Cyclic Diguanylate Interfere with Beneficial Bacterial Colonization. MBio 13:e0167122.

37. Nyholm SV, Stabb EV, Ruby EG, McFall-Ngai MJ. 2000. Establishment of an animal-bacterial association: recruiting symbiotic vibrios from the environment. Proc Natl Acad Sci U S A 97:10231–10235.

38. Yip ES, Geszvain K, DeLoney-Marino CR, Visick KL. 2006. The symbiosis regulator RscS controls the *syp* gene locus, biofilm formation and symbiotic aggregation by *Vibrio fischeri*. Mol Microbiol 62:1586–1600.

39. Visick KL. 2009. An intricate network of regulators controls biofilm formation and colonization by *Vibrio fischeri*. Mol Microbiol 74:782–789.

40. Ludvik DA, Bultman KM, Mandel MJ. 2021. Hybrid histidine kinase BinK represses *Vibrio fischeri* biofilm signaling at multiple developmental stages. J Bacteriol 203:e0015521.

41. Ruby EG, Asato LM. 1993. Growth and flagellation of *Vibrio fischeri* during initiation of the sepiolid squid light organ symbiosis. Arch Microbiol 159:160–167.

42. Yip ES, Grublesky BT, Hussa EA, Visick KL. 2005. A novel, conserved cluster of genes promotes symbiotic colonization and σ^{54}-dependent biofilm formation by *Vibrio fischeri*. Mol Microbiol 57:1485–1498.

43. Koehler S, Gaedeke R, Thompson C, Bongrand C, Visick KL, Ruby E, McFall-Ngai M. 2019. The model squid-vibrio symbiosis provides a window into the impact of strain- and

852 species-level differences during the initial stages of symbiont engagement. Environ
853 Microbiol 21:3269–3283.

854 44. Rotman ER, Bultman KM, Brooks JF 2nd, Gyllborg MC, Burgos HL, Wollenberg MS,
855 Mandel MJ. 2019. Natural strain variation reveals diverse biofilm regulation in squid-
856 colonizing *Vibrio fischeri*. J Bacteriol 201:e00033–19.

857 45. O'Shea TM, Klein AH, Geszvain K, Wolfe AJ, Visick KL. 2006. Diguanylate cyclases control
858 magnesium-dependent motility of *Vibrio fischeri*. J Bacteriol 188:8196–8205.

859 46. Bassis CM, Visick KL. 2010. The cyclic-di-GMP phosphodiesterase BinA negatively
860 regulates cellulose-containing biofilms in *Vibrio fischeri*. J Bacteriol 192:1269–1278.

861 47. Christensen DG, Marsden AE, Hodge-Hanson K, Essock-Burns T, Visick KL. 2020. LapG
862 mediates biofilm dispersal in *Vibrio fischeri* by controlling maintenance of the VCBS-
863 containing adhesin LapV. Mol Microbiol 114:742–761.

864 48. Tischler AH, Vanek ME, Peterson N, Visick KL. 2021. Calcium-Responsive Diguanylate
865 Cyclase CasA Drives Cellulose-Dependent Biofilm Formation and Inhibits Motility in *Vibrio*
866 *fischeri*. MBio 12:e0257321.

867 49. Ruby EG, Urbanowski M, Campbell J, Dunn A, Faini M, Gunsalus R, Lostroh P, Lupp C,
868 McCann J, Millikan D, Schaefer A, Stabb E, Stevens A, Visick K, Whistler C, Greenberg
869 EP. 2005. Complete genome sequence of *Vibrio fischeri*: a symbiotic bacterium with
870 pathogenic congeners. Proc Natl Acad Sci U S A 102:3004–3009.

871 50. Mandel MJ, Stabb EV, Ruby EG. 2008. Comparative genomics-based investigation of
872 resequencing targets in *Vibrio fischeri*: focus on point miscalls and artefactual expansions.
873 BMC Genomics 9:138.

874 51. Povolotsky TL, Hengge R. 2016. Genome-based comparison of cyclic di-GMP signaling in
875 pathogenic and commensal *Escherichia coli* strains. J Bacteriol 198:111–126.

876 52. Conner JG, Zamorano-Sánchez D, Park JH, Sondermann H, Yildiz FH. 2017. The ins and
877 outs of cyclic di-GMP signaling in *Vibrio cholerae*. Curr Opin Microbiol 36:20–29.

878 53. Wolfe AJ, Visick KL. 2010. The Second Messenger Cyclic Di-GMP. American Society for
879 Microbiology Press.

880 54. Shrestha P, Razvi A, Fung BL, Eichinger SJ, Visick KL. 2022. Mutational analysis of *Vibrio*
881 *fischeri* c-di-GMP-modulating genes reveals complex regulation of motility. J Bacteriol
882 e0010922.

883 55. Dial CN, Eichinger SJ, Foxall R, Corcoran CJ, Tischler AH, Bolz RM, Whistler CA, Visick
884 KL. 2021. Quorum Sensing and Cyclic di-GMP Exert Control Over Motility of *Vibrio fischeri*
885 KB2B1. Front Microbiol 12:690459.

886 56. Brooks JF 2nd, Gyllborg MC, Cronin DC, Quillin SJ, Mallama CA, Foxall R, Whistler C,
887 Goodman AL, Mandel MJ. 2014. Global discovery of colonization determinants in the squid
888 symbiont *Vibrio fischeri*. Proc Natl Acad Sci U S A 111:17284–17289.

889 57. Beyhan S, Yildiz FH. 2007. Smooth to rugose phase variation in *Vibrio cholerae* can be
890 mediated by a single nucleotide change that targets c-di-GMP signalling pathway. Mol
891 Microbiol 63:995–1007.

892 58. Lim B, Beyhan S, Yildiz FH. 2007. Regulation of Vibrio polysaccharide synthesis and
893 virulence factor production by CdgC, a GGDEF-EAL domain protein, in *Vibrio cholerae*. J
894 Bacteriol 189:717–729.

895 59. Waters CM, Lu W, Rabinowitz JD, Bassler BL. 2008. Quorum sensing controls biofilm

formation in *Vibrio cholerae* through modulation of cyclic di-GMP levels and repression of *vpsT*. J Bacteriol 190:2527–2536.

60. Hammer BK, Bassler BL. 2009. Distinct sensory pathways in *Vibrio cholerae* El Tor and classical biotypes modulate cyclic dimeric GMP levels to control biofilm formation. J Bacteriol 191:169–177.

61. Hunter JL, Severin GB, Koestler BJ, Waters CM. 2014. The *Vibrio cholerae* diguanylate cyclase VCA0965 has an AGDEF active site and synthesizes cyclic di-GMP. BMC Microbiol 14:22.

62. Kirillina O, Fetherston JD, Bobrov AG, Abney J, Perry RD. 2004. HmsP, a putative phosphodiesterase, and HmsT, a putative diguanylate cyclase, control Hms-dependent biofilm formation in *Yersinia pestis*. Mol Microbiol 54:75–88.

63. Purcell EB, McKee RW, McBride SM, Waters CM, Tamayo R. 2012. Cyclic diguanylate inversely regulates motility and aggregation in *Clostridium difficile*. J Bacteriol 194:3307–3316.

64. Edmunds AC, Castiblanco LF, Sundin GW, Waters CM. 2013. Cyclic Di-GMP modulates the disease progression of *Erwinia amylovora*. J Bacteriol 195:2155–2165.

65. Dunn AK, Millikan DS, Adin DM, Bose JL, Stabb EV. 2006. New *rfp*- and pES213-derived tools for analyzing symbiotic *Vibrio fischeri* reveal patterns of infection and *lux* expression in situ. Appl Environ Microbiol 72:802–810.

66. Spurbeck RR, Tarrien RJ, Mobley HLT. 2012. Enzymatically active and inactive phosphodiesterases and diguanylate cyclases are involved in regulation of Motility or sessility in *Escherichia coli* CFT073. MBio 3:e00307–12.

67. Sloup RE, Konal AE, Severin GB, Korir ML, Bagdasarian MM, Bagdasarian M, Waters CM. 2017. Cyclic Di-GMP and VpsR Induce the Expression of Type II Secretion in *Vibrio cholerae*. J Bacteriol 199:e00106-17.

68. Pursley BR, Maiden MM, Hsieh M-L, Fernandez NL, Severin GB, Waters CM. 2018. Cyclic di-GMP Regulates TfoY in *Vibrio cholerae* To Control Motility by both Transcriptional and Posttranscriptional Mechanisms. J Bacteriol 200:e00578-17.

69. Fernandez NL, Hsueh BY, Nhu NTQ, Franklin JL, Dufour YS, Waters CM. 2020. *Vibrio cholerae* adapts to sessile and motile lifestyles by cyclic di-GMP regulation of cell shape. Proc Natl Acad Sci U S A 117:29046–29054.

70. O'Shea TM, Deloney-Marino CR, Shibata S, Aizawa S-I, Wolfe AJ, Visick KL. 2005. Magnesium promotes flagellation of *Vibrio fischeri*. J Bacteriol 187:2058–2065.

71. Zamorano-Sánchez D, Xian W, Lee CK, Salinas M, Thongsomboon W, Cegelski L, Wong GCL, Yildiz FH. 2019. Functional Specialization in *Vibrio cholerae* Diguanylate Cyclases: Distinct Modes of Motility Suppression and c-di-GMP Production. MBio 10:e00670–19.

72. Beyhan S, Odell LS, Yildiz FH. 2008. Identification and characterization of cyclic diguanylate signaling systems controlling rugosity in *Vibrio cholerae*. J Bacteriol 190:7392–7405.

73. Yang C-Y, Chin K-H, Chuah ML-C, Liang Z-X, Wang AH-J, Chou S-H. 2011. The structure and inhibition of a GGDEF diguanylate cyclase complexed with $(c\text{-di-GMP})_2$ at the active site. Acta Crystallogr D Biol Crystallogr 67:997–1008.

74. Rao F, Yang Y, Qi Y, Liang Z-X. 2008. Catalytic Mechanism of Cyclic Di-GMP-Specific Phosphodiesterase: a Study of the EAL Domain-Containing RocR from *Pseudomonas aeruginosa*. J Bacteriol 190:3622–3631.

941 75. El Mouali Y, Kim H, Ahmad I, Brauner A, Liu Y, Skurnik M, Galperin MY, Römling U. 2017.
942 Stand-Alone EAL Domain Proteins Form a Distinct Subclass of EAL Proteins Involved in
943 Regulation of Cell Motility and Biofilm Formation in Enterobacteria. J Bacteriol 199:e00179-
944 17.

945 76. Cockerell SR, Rutkovsky AC, Zayner JP, Cooper RE, Porter LR, Pendergraft SS, Parker
946 ZM, McGinnis MW, Karatan E. 2014. *Vibrio cholerae* NspS, a homologue of ABC-type
947 periplasmic solute binding proteins, facilitates transduction of polyamine signals
948 independent of their transport. Microbiology 160:832–843.

949 77. Bridges AA, Prentice JA, Fei C, Wingreen NS, Bassler BL. 2022. Quantitative input–output
950 dynamics of a c-di-GMP signal transduction cascade in *Vibrio cholerae*. PLoS Biol
951 20:e3001585.

952 78. Dahlstrom KM, Collins AJ, Doing G, Taroni JN, Gauvin TJ, Greene CS, Hogan DA, O'Toole
953 GA. 2018. A multimodal strategy used by a large c-di-GMP network. J Bacteriol
954 200:e00703-17.

955 79. Kaczmarczyk A, van Vliet S, Jakob RP, Teixeira RD, Scheidat I, Reinders A, Klotz A, Maier
956 T, Jenal U. 2024. A genetically encoded biosensor to monitor dynamic changes of c-di-
957 GMP with high temporal resolution. Nat Commun 15:3920.

958 80. Graf J, Dunlap PV, Ruby EG. 1994. Effect of transposon-induced motility mutations on
959 colonization of the host light organ by *Vibrio fischeri*. J Bacteriol 176:6986–6991.

960 81. Visick KL, Ruby EG. 2006. *Vibrio fischeri* and its host: it takes two to tango. Curr Opin
961 Microbiol 9:632–638.

962 82. Mandel MJ, Schaefer AL, Brennan CA, Heath-Heckman EAC, Deloney-Marino CR, McFall-
963 Ngai MJ, Ruby EG. 2012. Squid-derived chitin oligosaccharides are a chemotactic signal

964 during colonization by *Vibrio fischeri*. Appl Environ Microbiol 78:4620–4626.

965 83. Brennan CA, DeLoney-Marino CR, Mandel MJ. 2013. Chemoreceptor VfcA mediates amino
966 acid chemotaxis in *Vibrio fischeri*. Appl Environ Microbiol 79:1889–1896.

967 84. Stabb EV, Ruby EG. 2002. RP4-based plasmids for conjugation between *Escherichia coli*
968 and members of the Vibrionaceae. Methods Enzymol 358:413–426.

969 85. Christensen DG, Visick KL. 2020. *Vibrio fischeri*: Laboratory Cultivation, Storage, and
970 Common Phenotypic Assays. Curr Protoc Microbiol 57:e103.

971 86. Visick KL, Hodge-Hanson KM, Tischler AH, Bennett AK, Mastrodomenico V. 2018. Tools
972 for rapid genetic engineering of *Vibrio fischeri*. Appl Environ Microbiol 84:e00850–18.

973 87. Boettcher KJ, Ruby EG. 1990. Depressed light emission by symbiotic *Vibrio fischeri* of the
974 sepiolid squid *Euprymna scolopes*. J Bacteriol 172:3701–3706.

975

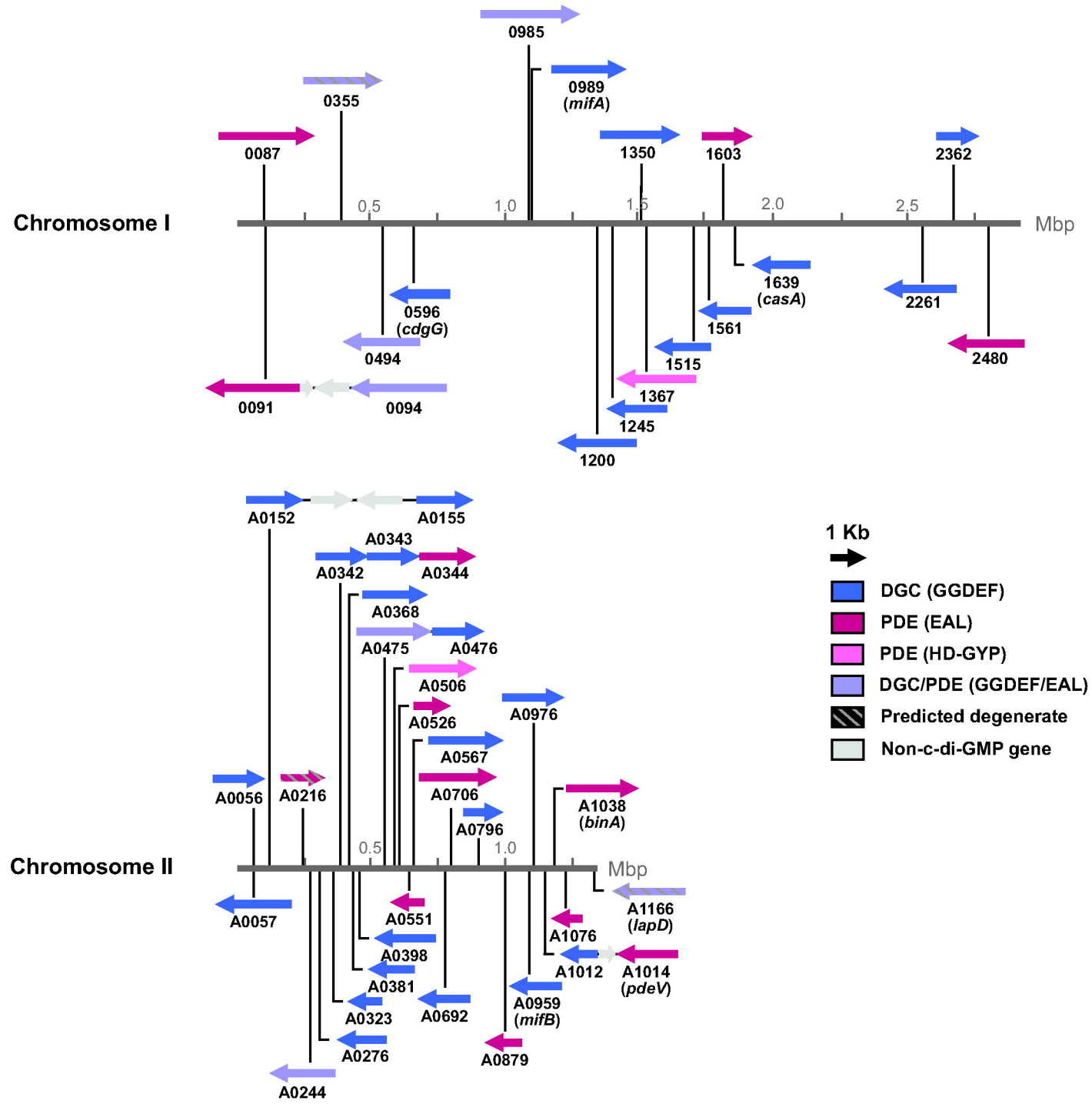

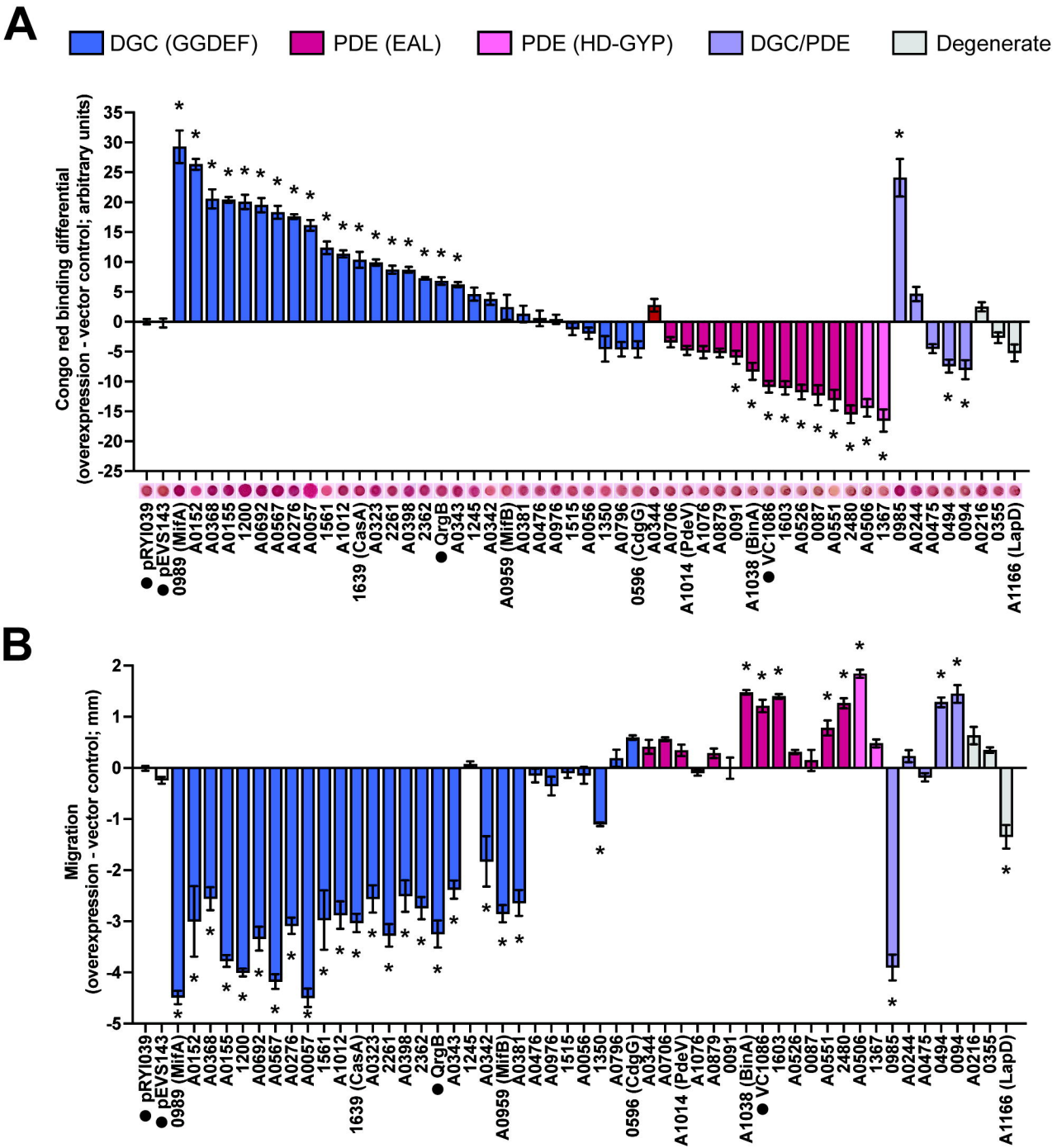
A
DGC (GGDEF)
PDE (EAL)
PDE (HD-GYP)
DGC/PDE
Degenerate
Congo red binding differential
(overexpression - vector control; arbitrary units)
35
30
25
20
15
10
5
0
-5
-10
-15
-20
-25
pRY1039
pEVS143
0989 (MifA)
A0152
A0368
A0155
1200
A0692
A0567
A0276
A0057
1561
A1012
1639 (CasA)
A0323
2261
A0398
2362
QrgB
A0343
1245
A0342
A0959 (MifB)
A0381
A0476
A0976
1515
A0056
1350
A0796
0596 (CdgG)
A0344
A0706
A1014 (PdeV)
A1076
A0879
0091
A1038 (BinA)
VC1086
1603
A0526
0087
A0551
2480
A0506
1367
0985
A0244
A0475
0494
0094
A0216
0355
A1166 (LapD)
B
Migration
(overexpression - vector control; mm)
2
1
0
-1
-2
-3
-4
-5
pRY1039
pEVS143
0989 (MifA)
A0152
A0368
A0155
1200
A0692
A0567
A0276
A0057
1561
A1012
1639 (CasA)
A0323
2261
A0398
2362
QrgB
A0343
1245
A0342
A0959 (MifB)
A0381
A0476
A0976
1515
A0056
1350
A0796
0596 (CdgG)
A0344
A0706
A1014 (PdeV)
A1076
A0879
0091
A1038 (BinA)
VC1086
1603
A0526
0087
A0551
2480
A0506
1367
0985
A0244
A0475
0494
0094
A0216
0355
A1166 (LapD)

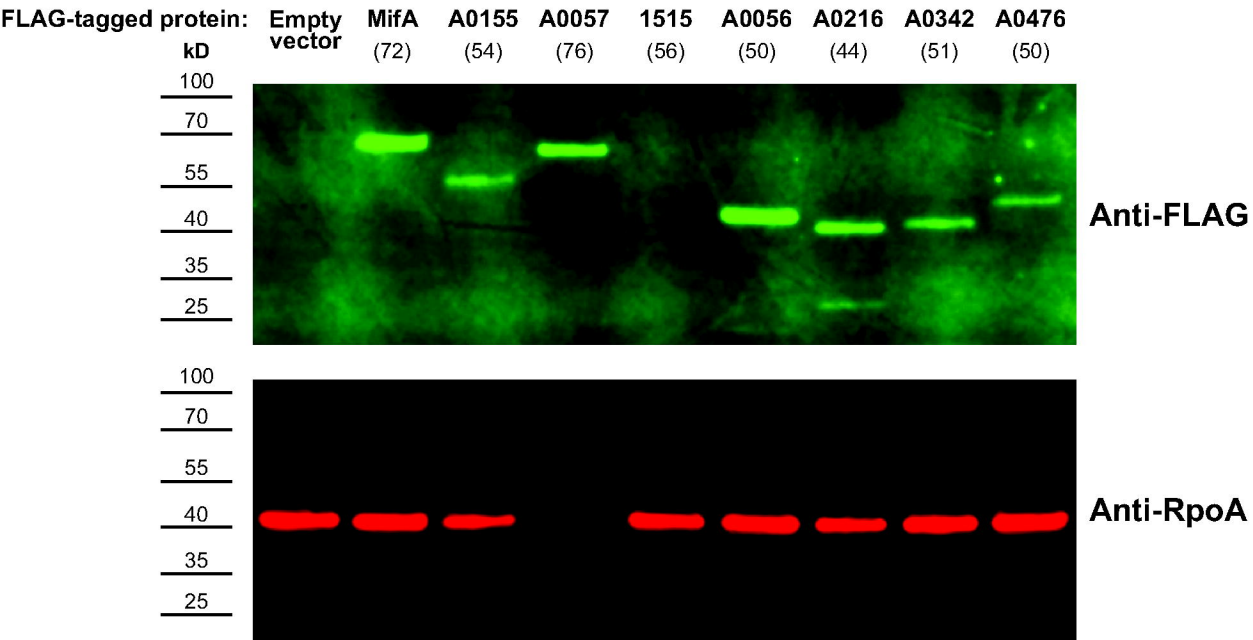

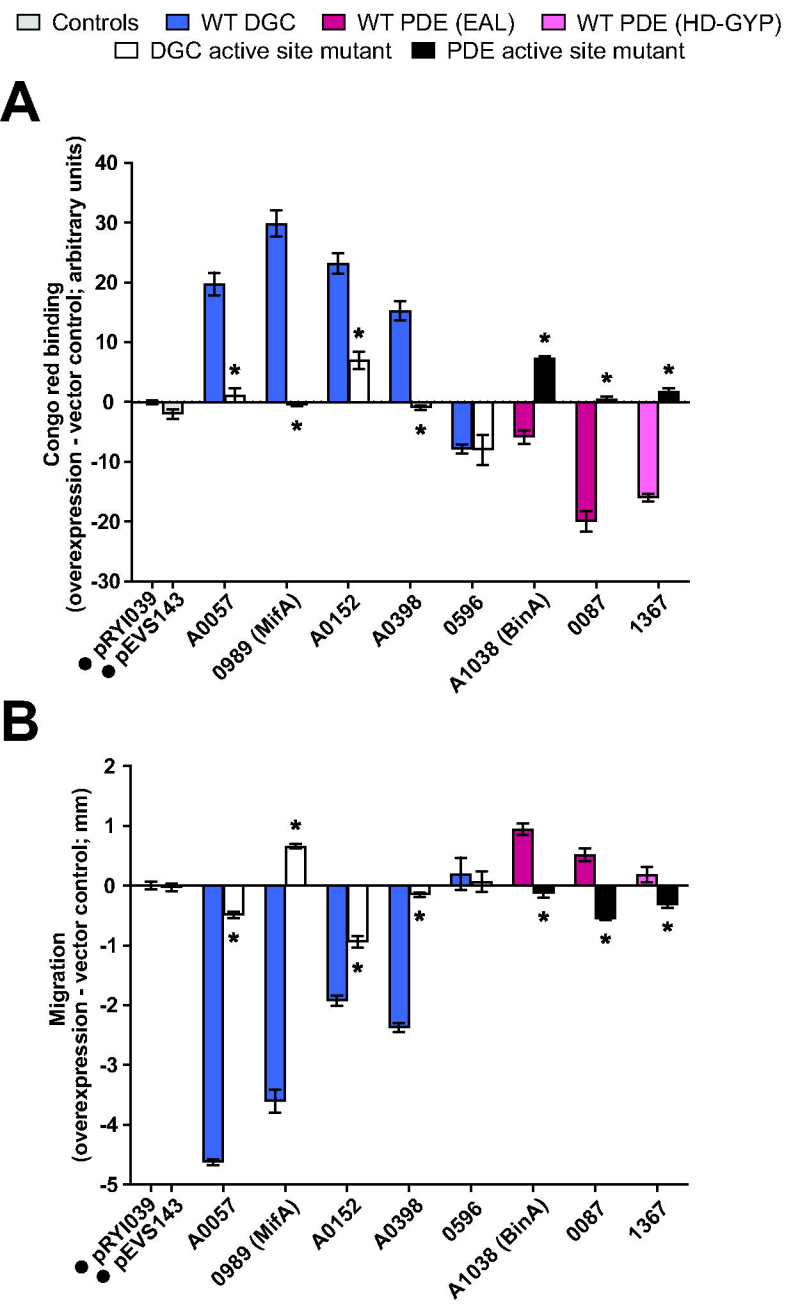

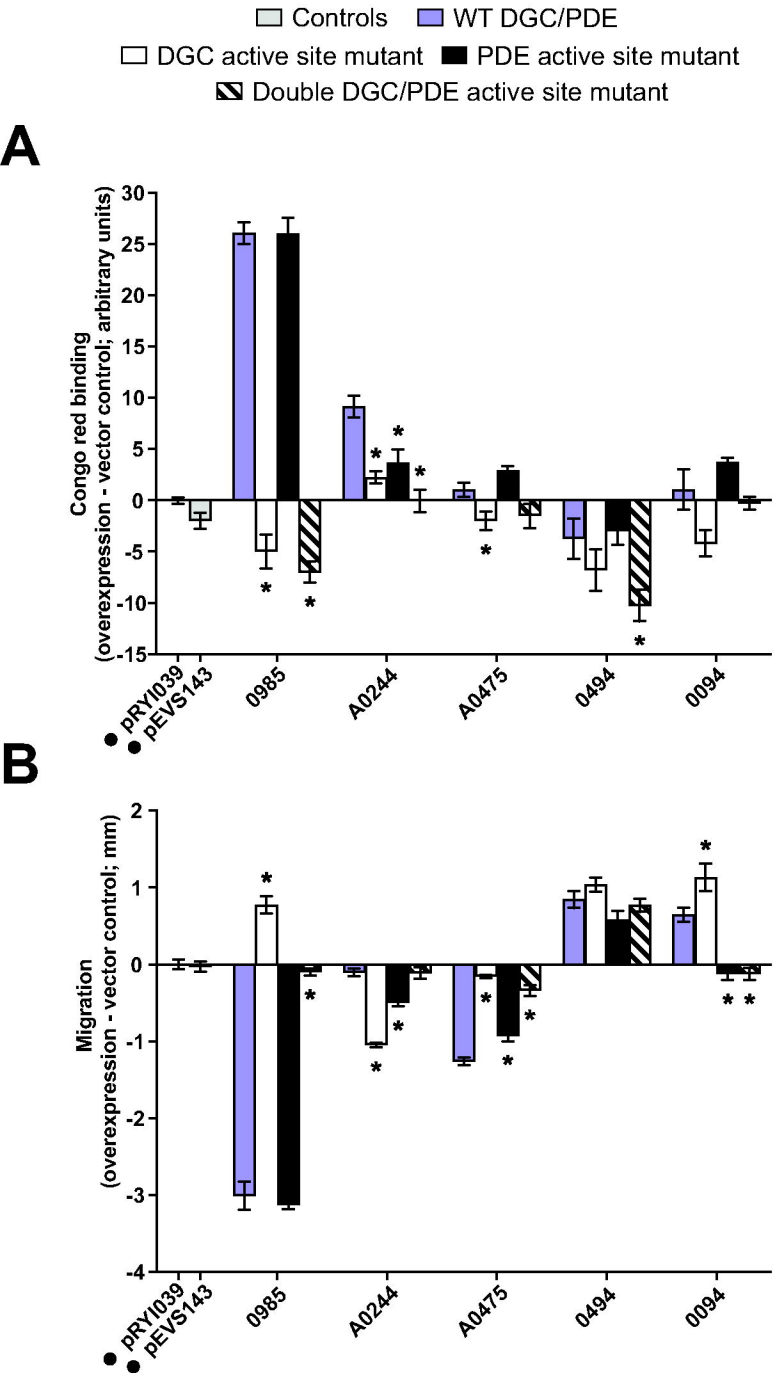

		Overexpression[a]				Deletion[b]		
			Motility			Motility		
	Protein	CR	TBS	Mg	Ca	TBS	Mg	Ca
DGCs (GGDEF)	0596 (CdgG)					-	-	-
	0989 (MifA)	+	-	-	-	+		+
	1200	+	-	-	-	+		+
	1245							
	1350		-					
	1515							
	1561	+	-	-	-			
	1639 (CasA)	+	-	-	-			+
	2261	+	-	-		+		
	2362	+	-	-	-			
	A0056							
	A0057	+	-	-	-			
	A0152	+	-	-	-			
	A0155	+	-	-	-			+
	A0276	+	-	-	-			+
	A0323	+	-	-	-			
	A0342		-	-	-			
	A0343	+	-	-	-			
	A0368	+	-	-	-	-		
	A0381		-	-	-	+		+
	A0398	+	-	-	-			
	A0476							-
	A0567	+	-	-	-			
	A0692	+	-	-	-			
	A0796							
	A0959 (MifB)		-	-	-	+	+	+
	A0976				+			-
	A1012	+	-	-	-			
	QrgB	+	-	-	-	N/A		
PDEs (EAL)	0087	-						
	0091	-						
	1603	-	+		+	-	-	-
	2480	-	+		+	-	-	-
	A0344				+			
	A0526	-				-	-	-
	A0551	-	+					
	A0706							
	A0879							
	A1014 (PdeV)							
	A1038 (BinA)	-	+		+			
	A1076							
	VC1086	-	+		+	N/A		
PDEs (HD-GYP)	1367	-						
	A0506	-	+		+			
DGC/PDEs	0094	-	+		+			-
	0494	-	+		+	-	-	-
	0985	+	-		-	+		
	A0244							
	A0475							
Degenerate	0355							-
	A0216							
	A1166 (LapD)		-	-				